Molecular Biology of the Cell
Vol. 12, 2497–2518, August 2001

Bud8p and Bud9p, Proteins That May Mark the Sites for Bipolar Budding in Yeast[V]

Heidi A. Harkins,* Nicolas Pagé,‡# Laura R. Schenkman,*† Claudio De Virgilio,*§ Sidney Shaw,*‖ Howard Bussey,‡ and John R. Pringle*†¶

*Department of Biology and †Program in Molecular Biology and Biotechnology, University of North Carolina, Chapel Hill, North Carolina 27599; and ‡Department of Biology, McGill University, Montreal H3A 1B1, Canada

Submitted November 7, 2000; Revised April 10, 2001; Accepted April 25, 2001
Monitoring Editor: David Drubin

The bipolar budding pattern of **a**/α *Saccharomyces cerevisiae* cells appears to depend on persistent spatial markers in the cell cortex at the two poles of the cell. Previous analysis of mutants with specific defects in bipolar budding identified *BUD8* and *BUD9* as potentially encoding components of the markers at the poles distal and proximal to the birth scar, respectively. Further genetic analysis reported here supports this hypothesis. Mutants deleted for *BUD8* or *BUD9* grow normally but bud exclusively from the proximal and distal poles, respectively, and the double-mutant phenotype suggests that the bipolar budding pathway has been totally disabled. Moreover, overexpression of these genes can cause either an increased bias for budding at the distal (*BUD8*) or proximal (*BUD9*) pole or a randomization of bud position, depending on the level of expression. The structures and localizations of Bud8p and Bud9p are also consistent with their postulated roles as cortical markers. Both proteins appear to be integral membrane proteins of the plasma membrane, and they have very similar overall structures, with long N-terminal domains that are both *N*- and *O*-glycosylated followed by a pair of putative transmembrane domains surrounding a short hydrophilic domain that is presumably cytoplasmic. The putative transmembrane and cytoplasmic domains of the two proteins are very similar in sequence. When Bud8p and Bud9p were localized by immunofluorescence and tagging with GFP, each protein was found predominantly in the expected location, with Bud8p at presumptive bud sites, bud tips, and the distal poles of daughter cells and Bud9p at the necks of large-budded cells and the proximal poles of daughter cells. Bud8p localized approximately normally in several mutants in which daughter cells are competent to form their first buds at the distal pole, but it was not detected in a *bni1* mutant, in which such distal-pole budding is lost. Surprisingly, Bud8p localization to the presumptive bud site and bud tip also depends on actin but is independent of the septins.

INTRODUCTION

A central feature of morphogenesis in many types of cells is cell polarization, which involves the asymmetric organization of the cytoskeleton, secretory system, and plasma membrane components along an appropriate axis (Drubin and Nelson, 1996). In the budding yeast *Saccharomyces cerevisiae*, such polarization allows asymmetric growth to form a bud, which becomes the daughter cell. An important feature of cell polarization is the selection of an appropriate axis. In *S. cerevisiae*, axis selection is manifested in the selection of bud sites, which occurs in two different patterns depending on the mating type of the cells (Freifelder, 1960; Hicks *et al.*, 1977; Chant and Pringle, 1995). In the axial pattern, as seen in *MAT**a*** or *MAT*α cells (such as normal haploids), the daughter cell's first bud forms adjacent to the division site (as marked by the birth scar), and each subsequent bud forms adjacent to the immediately preceding bud site (as marked by the bud scar). This pattern appears to depend on a transient cortical marker that involves the Bud3p, Bud4p, and Axl2p/Bud10p/Sro4p proteins (Chant *et al.*, 1995;

[V] Online version of this article contains video material for Figure 9. Online version is available at www.molbiolcell.org.

Present addresses: #Swiss Institute for Experimental Cancer Research (ISREC), 1066 Epalinges, Switzerland; §Botanisches Institut der Universität Basel, CH-4056 Basel, Switzerland; ‖Department of Biological Sciences, Stanford University, Stanford, CA 94305.
¶ Corresponding author. E-mail: jpringle@email.unc.edu.

Table 1. *S. cerevisiae* strains used in this study

Strain	Genotype[a]	Source
YEF473	**a**/α *his3-Δ200/his3-Δ200 leu2-Δ1/leu2-Δ1 lys2-801/lys2-801 trp1-Δ63/trp1-Δ63 ura3-52/ura3-52*	Bi and Pringle, 1996
YEF473A	**a** *his3-Δ200 leu2-Δ1 lys2-801 trp1-Δ63 ura3-52*	Segregant from YEF473
YEF473B	α *his3-Δ200 leu2-Δ1 lys2-801 trp1-Δ63 ura3-52*	Segregant from YEF473
SEY6210	α *leu2-3,112 ura3-52 his3-Δ200 trp1-Δ901 lys2-801 suc2-Δ9*	Robinson *et al.*, 1988
SEY6210D	**a**/α *leu2-3,112/leu2-3,112 ura3-52/ura3-52 his3-Δ200/his3-Δ200 trp1-Δ901/trp1-Δ901 lys2-801/lys2-801 suc2-Δ9/suc2-Δ9*	Roemer and Bussey, 1991[b]
SEY6211	**a** *leu2-3,112 ura3-52 his3-Δ200 trp1-Δ901 ade2-101 suc2-Δ9*	Robinson *et al.*, 1988
HAB880	as SEY6210 except *mnn9::kanMX2*	Shahinian *et al.*, 1998
HAB881	as SEY6210 except *och1::kanMX2*	Shahinian *et al.*, 1998
HAB897	as SEY6210 except **a** *pmt1::HIS3*	Lussier *et al.*, 1995
HAB898	as SEY6210 except *pmt2::LEU2*	Lussier *et al.*, 1995
HAB899	as SEY6210 except **a** *pmt1::HIS3 pmt2::LEU2*	Lussier *et al.*, 1995
Pmt2/4	*pmt2::LEU2 pmt4::TRP1* (SEY6210/SEY6211 background)	W. Tanner
Pmt1/3	*pmt1::URA3 pmt3::HIS3* (SEY6210/SEY6211 background)	W. Tanner
Pmt1/4	*pmt1::URA3 pmt4::TRP1* (SEY6210/SEY6211 background)	W. Tanner
Pmt1/5	*pmt1::HIS3 pmt5::URA3* (SEY6210/SEY6211 background)	W. Tanner
Pmt1/6	*pmt1::HIS3 pmt6::URA3* (SEY6210/SEY6211 background)	W. Tanner
Pmt1/3/4	*pmt1::URA3 pmt3::HIS3 pmt4::TRP1* (SEY6210/SEY6211 background)	W. Tanner
Pmt3/4	*pmt3::HIS3 pmt4::TRP1* (SEY6210/SEY6211 background)	W. Tanner
YJZ358	as YEF473 except *bud6-Δ3/bud6-Δ3*[c]	Amberg *et al.*, 1997
YJZ426	as YEF473A except *bni1Δ::HIS3*[d]	J. Zahner
YJZ427	as YEF473B except *bni1Δ::HIS3*[d]	J. Zahner
YS148	**a**/α *ade2-101/ade2-101 HIS3/his3-Δ200 leu2Δ98/leu2Δ98 lys2-801/lys2-801 trp1Δ/trp1Δ ura3-52/ura3-52 spa2-Δ3::URA3/spa2-Δ3::URA3*	M. Snyder (Gehrung and Snyder, 1990)
AB324	**a**/α *his3/his3 leu2/leu2 ura3/ura3 rsr1::URA3/rsr1::URA3*	A. Bender (Bender and Pringle, 1989)
ML130	as YEF473A except *bar1Δ*	M. Longtine
LSY192	as YEF473A except *cdc12-6 bar1Δ*	This study[e]
LSY42	as YEF473 except *BUD9/P_{GAL}-GFP-BUD9*[f]	See text
LSY41	as YEF473 except *P_{GAL}-GFP-BUD9/P_{GAL}-GFP-BUD9*[f]	See text
YHH141	α *his4 leu2 trp1 ura3 bud9-1 bud3::TRP1*	This study[g]
YHH145	α *his4 leu2 trp1 ura3 bud8-1 bud3::TRP1*	This study[g]
YHH273	**a**/α *leu2/leu2 trp/trp1 ura3/ura3 bud3::TRP1/bud3::TRP1 bud9-1/bud9-1*	This study[h]
YHH274	**a**/α *leu2/leu2 trp/trp1 ura3/ura3 bud3::TRP1/bud3::TRP1 bud8-1/bud8-1*	This study[h]
YHH312	**a** *his4 leu2 trp1 ura3 bud9-1*	This study[i]
YHH315	**a** *his4 leu2 trp1 ura3 bud8-1*	This study[j]
YHH387	as YEF473 except *BUD8/bud8-Δ1*	See text
YHH391	as YEF473B except *bud8-Δ1*	Segregant from YHH387
YHH394	as YEF473A except *bud8-Δ1*	Segregant from YHH387
YHH399	**a**/α *HIS3/his3-Δ200 his4/HIS4 leu2/leu2-Δ1 LYS2/lys2-801 trp1/trp1-Δ63 ura3/ura3-52 bud8-1/bud8-Δ1*	YHH315 × YHH391
YHH415	as YEF473 except *bud8-Δ1/bud8-Δ1*	YHH391 × YHH394
YHH514	as YEF473 except *bud8-Δ1/bud8-Δ1 URA3:HA-BUD8/URA3:HA-BUD8*	See text
YHH529	as YEF473 except *bud8-Δ1/bud8-Δ1 URA3:GFP-BUD8/URA3:GFP-BUD8*[f]	See text
YHH610	as YEF473 except *BUD9/bud9-Δ1*	See text
YHH613	as YEF473A except *bud9-Δ1*	Segregant from YHH610
YHH614	as YEF473B except *bud9-Δ1*	Segregant from YHH610
YHH615	as YEF473 except *bud9-Δ1/bud9-Δ1*	YHH613 × YHH614
YHH616	as YEF473 except *bud9-1/bud9-Δ1*	YHH312 × YHH614
YHH625	as YEF473 except *bud8-Δ1/bud8-Δ1 bud9-Δ1/bud9-Δ1*	YHH631 × YHH632
YHH631	as YEF473B except *bud8-Δ1 bud9-Δ1*	Segregant from YHH391 × YHH613
YHH632	as YEF473A except *bud8-Δ1 bud9-Δ1*	Segregant from YHH391 × YHH613
YHH759	**a**/α *his4/his4 leu2/leu2 trp1/trp1 ura3/ura3 bud5::URA3/bud5::URA3*	This study[k]
YHH772	as YEF473 except *bud3Δ::HIS3/bud3Δ::HIS3 bud8-Δ1/bud8-Δ1 bud9-Δ1/bud9-Δ1*	This study[l]
YHH782	**a**/α *ade2/ade2 ade3/ade3 his3/his3 leu2/leu2 lys2/lys2 trp1/trp1 ura3/ura3 bud2Δ::TRP1/bud2Δ::TRP1*	This study[m]

Table 1. (Continued)

Strain	Genotype[a]	Source
YHH800	as YEF473 except *bni1*Δ*::HIS3/bni1*Δ*::HIS3* [p39L12] [YEpGFP-BUD8]	This study[n]
YHH802	as YEF473 except *bni1*Δ*::HIS3/bni1*Δ*::HIS3* [YEpGFP-BUD8]	This study[n]

[a] Plasmids are indicated in square brackets.

[b] The strain created by *HO*-induced diploidization of SEY6210.

[c] This allele has previously been referred to as *aip3-*Δ*3::TRP1*.

[d] A precise replacement of the *BNI1* open reading frame by *HIS3*.

[e] Segregant from the cross of ML130 to a strain generated by seven backcrosses of a *cdc12-6* mutation (Adams and Pringle, 1984) into YEF473A.

[f] The *GFP* sequences encode GFP with the S65T substitution.

[g] Segregants from crosses of YHH94 and YHH98 (Zahner *et al.*, 1996), respectively, to YHH17 (a segregant from the same tetrad as YHH16 [Zahner *et al.*, 1996]).

[h] Derived by mating other segregants from the crosses described in note g.

[i] Segregant from a cross of YHH141 to YHH114 (Zahner *et al.*, 1996).

[j] Segregant from a cross of YHH145 to YHH137 (Zahner *et al.*, 1996).

[k] A segregant from a cross of JC206 [similar to strain 205 (Chant *et al.*, 1991)] to YEF473A was mated to a segregant from a cross of JC207 (also similar to strain 205) to YEF473B, yielding YHH759.

[l] Derived by mating segregants from a cross of YHH632 to DDY206-3A (provided by D. DeMarini; it carries a complete deletion of the *BUD3* open reading frame in the YEF473B background).

[m] Derived by mating HPy138 to HPy143a (both from H.-O. Park).

[n] Strains YJZ426 × YJZ427 were mated after transforming with plasmids p39L12 and p39C (Table 2), respectively. A subclone of the resulting diploid that had lost p39C was identified and transformed with YEpGFP-BUD8, yielding strain YHH800. A subclone of YHH800 that had lost p39L12 was named YHH802.

Halme *et al.*, 1996; Roemer *et al.*, 1996a; Sanders and Herskowitz, 1996); this marker is deposited at the mother-bud neck, and then distributed to the division site on both mother and daughter cells, during each cell cycle.

In contrast, the bipolar pattern, as seen in *MAT***a***/MAT*α cells (such as normal diploids), appears to depend on persistent markers that are deposited at both the birth-scar-distal and birth-scar-proximal poles of the daughter cell, as well as at the division site on the mother cell (Chant and Pringle, 1995). These markers can direct bud formation to the marked site either in the next cell cycle or in a later one. A screen for mutants with normal axial bud-site selection but defective bipolar bud-site selection led to the identification of the *BUD8* and *BUD9* genes, which have mutant phenotypes suggesting that they might encode components of the markers at the distal and proximal poles of the daughter cell, respectively (Zahner *et al.*, 1996). Specifically, the *bud8* mutants bud almost exclusively around the proximal pole, whereas the *bud9* mutants bud almost exclusively around the distal pole. We report here the cloning of *BUD8* and *BUD9* and the initial molecular analyses of their products. These analyses suggest that Bud8p and Bud9p do indeed mark the opposite poles of the daughter cell. Both proteins contain large extracellular domains, which may anchor them in their specific locations by interacting with the cell wall, and short cytoplasmic domains. The cytoplasmic domains are very similar to each other in sequence and may provide the recognition sites for the Rsr1p/Bud2p/Bud5p GTPase signaling module, which appears to transmit the positional information from the axial and bipolar cortical markers to the proteins responsible for cell polarization (Pringle *et al.*, 1995; Roemer *et al.*, 1996b; Chant, 1999).

MATERIALS AND METHODS

Strains, Plasmids, Growth Conditions, and Genetic and Recombinant DNA Methods

Yeast strains used in this study are listed in Table 1; the construction of strains containing deletions and/or tagged genes is described below. Plasmids used in this study are listed in Table 2 or described where appropriate below. Cells were grown on YM-P or YPD rich liquid medium, solid YPD medium, synthetic complete (SC) medium lacking appropriate nutrients, or minimal medium plus casamino acids (Lillie and Pringle, 1980; Guthrie and Fink, 1991; Salmon *et al.*, 1998), as indicated; 2% glucose was used as carbon source except where noted. Cells were grown at 23°C except where noted. Cells expressing Bud8p or Bud9p tagged with the green fluorescent protein (GFP) were grown in the dark to minimize photobleaching.

For the experiments using α mating pheromone to produce synchronous populations of unbudded, G1-phase cells, α factor (Sigma Chemical Co., St. Louis, MO) was added (final concentration, 25 ng/ml) to cultures growing exponentially (~10^7 cells/ml) in SC-Leu medium. After 90 min, the cultures were diluted threefold with fresh SC-Leu medium that had been prewarmed to 37°C and contained 25 ng/ml α factor, and incubation was continued for 30 min at 37°C, at which point >90% of the cells were unbudded. Cells were collected by centrifugation at 2000 rpm for 5 min, resuspended in half the original volume of SC-Leu medium (without α factor) at 37°C, and incubated further at 37°C.

For the experiments using Latrunculin A (Lat A; Molecular Probes, Eugene, OR) to depolymerize F-actin, a preculture in 2×SC-

Table 2. Plasmids used in this study

Plasmid	Description	Source
pRS315	*CEN6 ARSH4 LEU2* (low copy)	Sikorski and Hieter, 1989
pRS316	*CEN6 ARSH4 URA3* (low copy)	Sikorski and Hieter, 1989
pRS425	*LEU2* (high copy)	Christianson *et al.*, 1992
pRS426	*URA3* (high copy)	Christianson *et al.*, 1992
YCplac111	*CEN4 ARS1 LEU2* (low copy)	Gietz and Sugino, 1988
YEplac181	*LEU2* (high copy)	Gietz and Sugino, 1988
YEplac195	*URA3* (high copy)	Gietz and Sugino, 1988
YIplac211	*URA3* (integrating)	Gietz and Sugino, 1988
YCpIF2	*CEN4 ARS1 LEU2* P_{GAL}	Foreman and Davis, 1994
YEp352-SUC2	*URA3 SUC2* (high copy)	Lussier *et al.*, 1996, 1997a
CB612-Kre1p-HA	*URA3* P_{ADH}-*HA-KRE1* (high copy)	Roemer and Bussey, 1995
YCpBUD8	*BUD8* in pRS316	See text
YEpBUD8	*BUD8* in YEplac181	See text
YCpGAL-BUD8	P_{GAL}-*BUD8* in YCpIF2	See text
YCpBUD9	*BUD9* in YCplac111	See text
YEpBUD9	*BUD9* in YEplac195	See text
YCpHA-BUD8	*HA-BUD8* in pRS315	See text
YEpHA-BUD8-5	*HA-BUD8* in pRS425	See text
YEpBUD8-6	*BUD8* in pRS426	See text
YEpHA-BUD8-6	*HA-BUD8* in pRS426	See text
YCpHA-BUD9	*HA-BUD9* in YCplac111	See text
YEpHA-BUD9	*HA-BUD9* in YEplac195	See text
YEpGFP-BUD8	*GFP-BUD8* in YEplac181[a]	See text
YEpGFP*-BUD8	*GFP-BUD8* in YEplac181[b]	See text
YCpGFP-BUD9	*GFP-BUD9* in YCplac111[a]	See text
YEpGFP-BUD9	*GFP-BUD9* in YEplac195[a]	See text
p39L12	*BNI1 URA3* (high copy)	H. Fares
p39C	*BNI1 LEU2* (low copy)	H. Fares

[a] The *GFP* sequences encode GFP with the S65T substitution.

[b] The *GFP* sequences encode GFP with the F64L, S65T, and V163A substitutions.

Leu medium (like SC-Leu, but with all ingredients at twice their normal concentrations) containing 0.2% glucose as carbon source was inoculated to ~10^6 cells/ml and incubated at 30°C for 48 h, at which point ~90% of the cells were unbudded. Cells were collected by centrifugation and reinoculated at ~1.5×10^7 cells/ml into SC-Leu medium containing 2% glucose at 23°C. Lat A (a 200-fold dilution of a 20 mM stock solution in dimethyl sulfoxide [DMSO]) or an equivalent amount of DMSO alone was added, and the cultures were incubated at 23°C.

Escherichia coli strains DH12S, DH5α, and DH10B (Life Technologies, Gaithersburg, MD) were used routinely as plasmid hosts and were grown under standard conditions (Sambrook *et al.*, 1989). Standard methods of yeast genetics and DNA manipulation (Sambrook *et al.*, 1989; Guthrie and Fink, 1991; Gietz *et al.*, 1992; Ausubel *et al.*, 1995) were used except where noted. Except where noted, enzymes were purchased from New England Biolabs (Beverly, MA). The polymerase chain reaction (PCR) used either Vent DNA polymerase or the Expand High Fidelity System (Roche Molecular Biochemicals, Indianapolis, IN). Oligonucleotide primers were from Integrated DNA Technologies (Coralville, IA). For physical mapping, ^{32}P-labeled DNA fragments were used to probe a filter carrying the ordered set of λ′ clones of yeast genomic DNA (Riles *et al.*, 1993; American Type Culture Collection, Rockville, MD).

Cloning and Sequencing of BUD8 *and* BUD9

BUD8 and *BUD9* were cloned by transforming strains YHH274 and YHH273 (Table 1) with an *S. cerevisiae* genomic DNA library in plasmid YCp50-LEU2 (kindly provided by F. Spencer and P. Hieter, Johns Hopkins University, Baltimore, MD). Transformants were stained with Calcofluor to visualize bud scars (see below) and examined as described previously (Zahner *et al.*, 1996) for complementation of the budding-pattern defects. Of 1700 transformants examined for strain YHH274, one showed a plasmid-dependent restoration of normal bipolar budding. Of 4032 transformants examined for strain YHH273, two showed a plasmid-dependent restoration of normal bipolar budding. Restriction mapping indicated that the two plasmids had similar or identical inserts.

For further analysis of *BUD8*, an ~3.0-kb *Bam*HI-*Xba*I fragment that proved to contain the entire *BUD8* open reading frame (ORF) plus 547 bp of upstream sequence and 608 bp of downstream sequence (Figure 1A) was subcloned into *Bam*HI/*Xba*I-digested pBluescript KS(+) (Stratagene, La Jolla, CA) to generate plasmid pKS-BUD8 and into *Bam*HI/*Xba*I-digested pRS316 to generate plasmid YCpBUD8. In addition, an ~2.5-kb *Hin*dIII-*Sca*I fragment from YCpBUD8 (containing the *BUD8* ORF plus 290 bp of upstream sequence and 391 bp of downstream sequence) was subcloned into *Hin*dIII/*Sma*I-digested YEplac181 to generate plasmid YEpBUD8. To construct a plasmid expressing *BUD8* under control of the *GAL1/10* promoter (P_{GAL}), site-directed mutagenesis was used to introduce a *Bam*HI site immediately upstream of the *BUD8* start codon and a *Hin*dIII site 141 bp downstream of the *BUD8* stop codon. To this end, the *Hin*dIII-*Sca*I fragment from pKS-BUD8 (see above) was subcloned into *Hin*dIII/*Sma*I-digested pALTER-1 (Promega, Madison, WI) to generate plasmid pALT-BUD8. Mutagenesis was then performed as recommended by Promega, using primers HH1 and HH2 (Table 3), to generate plasmid pALT-BUD8(B/H).

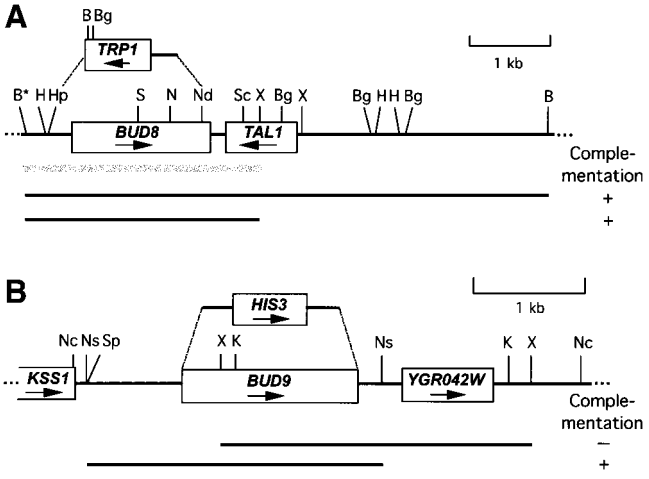

Figure 1. Structures of the *BUD8/YLR353W* (A) and *BUD9/YGR041W* (B) regions and of the *bud8-Δ1* and *bud9-Δ1* deletion alleles. Open boxes represent open reading frames; arrows indicate directions of transcription. Solid lines beneath the maps indicate DNA fragments tested (in the low-copy vector pRS316 or YCplac111) for complementation of the *bud8-1* or *bud9-1* phenotype in strain YHH274 or YHH273. Deletion alleles were constructed as described in the text. (A) Hatched line indicates the fragment used as probe for Southern blots. All sites are shown for restriction enzymes *Bam*HI (B), *Bgl*II (Bg), *Hin*dIII (H), *Hpa*I (Hp), *Nde*I (Nd), *Nhe*I (N), *Sal*I (S), *Sca*I (Sc), and *Xba*I (X). The *Bam*HI site indicated by B* may have been created by the fusion of a chromosomal *Sau*3A site to the vector *Bam*HI site during library construction. (B) All sites are shown for restriction enzymes *Kpn*I (K), *Nco*I (Nc), *Nsi*I (Ns), *Sph*I (Sp), and *Xba*I (X).

The *Bam*HI-*Hin*dIII fragment was then subcloned into *Bam*HI/*Hin*dIII-digested YCpIF2 to generate plasmid YCpGAL-BUD8.

For further analysis of *BUD9*, an ~2.7-kb *Nsi*I fragment that proved to contain the entire *BUD9* ORF plus 864 bp of upstream sequence and 192 bp of downstream sequence (Figure 1B) was subcloned into *Pst*I-digested YCplac111 to generate plasmid YCp-BUD9 and into *Pst*I-digested YEplac195 to generate plasmid YEp-BUD9.

To sequence *BUD8*, pKS-BUD8 (see above) was subjected to *Bal*31 nuclease treatment to generate a deletion series (Ausubel *et al.*, 1995). Both strands of the *BUD8* region were then sequenced from the *Bam*HI site to just beyond the *Sca*I site (Figure 1A) using the M13 primers and the Sequenase reagent kit (USB, Cleveland, OH) according to the manufacturer's instructions. To sequence *BUD9*, both strands of the ~2.7-kb *Nsi*I fragment in YCpBUD9 were sequenced by the University of North Carolina-Chapel Hill DNA Sequencing Facility with the use of sequentially generated primers. Comparison of our sequences to those from the genome project (all sequences can be accessed through the Saccharomyces Genome Database; see accession numbers given in RESULTS) revealed some discrepancies, some of which lead to changes in the predicted amino acid sequences (Figure 4A). These discrepancies may represent polymorphisms in the DNAs sequenced or errors in the various sequences.

Deletion and Tagging of BUD8 *and* BUD9

To delete *BUD8*, the ~1.2-kb *Sma*I-*Nde*I fragment containing *TRP1* from plasmid pJJ280 (equivalent to pJJ246 [Jones and Prakash, 1990]) was ligated into *Hpa*I/*Nde*I-digested pKS-BUD8 to generate plasmid pKS-TRP. This deletes *BUD8*-region sequences from 247 bp upstream of the *BUD8* start codon (no other gene overlaps this region) to 118 bp upstream of the *BUD8* stop codon (Figure 1A). The ~2.2-kb *Sma*I-*Sac*II fragment (both sites from the vector) from pKS-TRP was then used to transform strain YEF473. Trp^+ transformants were analyzed by Southern blotting after digestion of genomic DNA with *Bam*HI and *Bgl*II, using the *Bam*HI-*Xba*I fragment (Figure 1A) as probe. Strain YHH387 displayed the bands expected for a *BUD8/bud8-Δ1* heterozygote, and tetrad analysis showed the expected correlated segregation of Trp^+:Trp^- with the appropriate bands as detected by Southern blotting (our unpublished results).

The *BUD9* coding region was precisely deleted by the PCR method of Baudin *et al.* (1993), using *HIS3*-containing plasmid pRS303 (Sikorski and Hieter, 1989) as template and primers ΔBUD9-F and ΔBUD9-R (Table 3). The PCR product was transformed into strain YEF473, selecting for His^+. PCR using primers ΔBUD9-F and BUD9-R1 indicated that transformant YHH610 had one copy of *BUD9* replaced by *HIS3*, and tetrad analysis showed a 2:2 segregation of His^+:His^- (our unpublished results).

To create plasmids carrying *GFP* cassettes that could be used to tag *BUD8* and *BUD9*, the GFP ORF was amplified by PCR using primers GFP-F and GFP-R (Table 3) and plasmid pS65T-C1 (Clontech, Palo Alto, CA) as template. The PCR product was cut with *Eco*RI (sites included in the primers) and cloned into *Eco*RI-cut pBluescript KS(+), thus creating plasmid pKS-GFP^{S65T}, which encodes full-length GFP carrying the S65T substitution (Heim *et al.*, 1995). A series of three steps then generated plasmid pKS-GFP*. First, the *Msc*I-*Mfe*I fragment (both sites in the GFP ORF) of pKS-GFP^{S65T} was replaced by the corresponding fragment from a plasmid (kindly provided by C. Albright and H. McDonald, Vanderbilt University, Nashville, TN) that encodes GFP with both the F64L and S65T substitutions (Cormack *et al.*, 1996), thus creating plasmid pKS-$GFP^{F64L,S65T}$. Second, the *Nde*I-*Mfe*I fragment (both sites in the GFP ORF) of pKS-GFP^{S65T} was replaced by the corresponding fragment from plasmid pAFS135 (Straight *et al.*, 1998), which encodes GFP with the V163A substitution, thus creating plasmid pKS-$GFP^{S65T,V163A}$. Third, the *Pml*I-*Kpn*I fragment (former site downstream of GFP codon 65, latter site in the vector polylinker) of pKS-$GFP^{F64L,S65T}$ was replaced by the corresponding fragment from pKS-$GFP^{S65T,V163A}$, thus creating plasmid pKS-GFP*, which encodes GFP carrying the F64L, S65T, and V163A substitutions.

To tag Bud8p, the pALTER system, plasmid pALT-BUD8 (see above), and primer HH3 were used to introduce a *Not*I site immediately after the *BUD8* start codon. *Not*I fragments carrying sequences encoding three copies of the hemagglutinin epitope (HA; from plasmid pGTEP1 [Tyers *et al.*, 1993; Schneider *et al.*, 1995]) or GFP^{S65T} (from plasmid pKS-GFP^{S65T}; see above) were then inserted at the introduced *Not*I site. The *Hin*dIII-*Kpn*I fragments (latter site from the vector polylinker) from the resulting plasmids were then subcloned into *Hin*dIII/*Kpn*I-digested YIplac211. The resulting plasmids were linearized within *URA3* by digestion with *Apa*I and transformed into *bud8-Δ1* strains YHH391 and YHH394, selecting stable Ura^+ transformants. For each tagged *BUD8* allele, three different pairs of transformants were mated to check the budding pattern of ***a***/***α*** cells. The resulting diploids (including strains YHH514 and YHH529) displayed approximately normal bipolar budding (Figure 2, O and P; Figure 3, A–C), indicating that the HA-tagged and GFP-tagged Bud8p provided approximately normal Bud8p function. To construct additional *HA-BUD8* plasmids, the *Hin*dIII-*Sac*I fragment (latter site from the vector polylinker) carrying the tagged allele was subcloned from pALTER into *Hin*dIII/*Sac*I-digested pRS315 to generate plasmid YCpHA-BUD8. The same sites were then used to subclone the *HA-BUD8* fragment from YCpHA-BUD8 into pRS425 and pRS426, thus generating plasmids YEpHA-BUD8–5 and YEpHA-BUD8-6, respectively. Control plasmid YEpBUD8-6 was constructed by using the *Hin*dIII and *Sac*I sites (latter site from the vector) to subclone the fragment carrying untagged *BUD8* from YCpBUD8 into *Hin*dIII/*Sac*I-digested pRS426. To construct additional *GFP-BUD8* plasmids, the *Hin*dIII-*Kpn*I fragment (latter site from the vector polylinker) carrying the tagged allele was subcloned from pALTER into *Hin*dIII/*Kpn*I-digested YE-

Table 3. Oligonucleotide primers used for gene deletion, cloning, and tagging

Primer	Sequence
HH1	5′-TTCGTCTGATTGTATCATGGATCCACTTCATGTAGAATCGAA-3′[a]
HH2	5′-CCATGTCCTTATGCCGTTAAGCTTTCTTTTGATACTTACGGG-3′[a]
HH3	5′-ATCTTCGTCTGATTGTATGCGGCCGCCCATACTTCATGTAGAATCGAA-3′[b]
ΔBUD9-F	5′-TCACTACCTTTTTTTTTACAACAATTTCATTCTTCATCCTATGAAGATTGTACTGAGAGTGCACC-3′[c]
ΔBUD9-R	5′-ATAGAGAGTAGCAGGAAATCTTCGACGAGTAAGTCCAGCATGGAGCTGTGCGGTATTTCACACCG-3′[c]
BUD9-R1	5′-TCGCTATTCCAACGAATATGAGCTCTTGGTGTTGAG-3′[c]
GFP-F	5′-CCGCTAGCGAATTCAGGCGGCCGCATGGGTAAAGGAGAAGAACTTTTCACTGGAGTTGTC-3′[d]
GFP-R	5′-CGAAGCTGAATTCAAGCGGCCGCAGGATCCCTTGTATAGTTCATCCATGCCATGTGTAATCCC-3′[d]
LS8	5′-CCGTTGCCGATCCAGATG-3′[e]
LS10	5′-ACCTTTTTTTTTTACAACAATTTCATTCTTCATCCTATGAAGAATTCGAGCTCGTTTAAAC-3′[e]
LS11	5′-TTTCTGTCGTTATCGAAACATCTCTGGTTATTTTCGTCATTTTGTATAGTTCATCCATGC-3′[e]
LS33	5′-CCGCATCAGGCGCCATTC-3′[f]
LS34	5′-CGTGCGGCCGCACATTTCATAGGATGAAGAATGAA-3′[f]
LS35	5′-GAAATGTGCGGCCGCACGAAAATAACCAGAGATGTTTC-3′[f]
LS36	5′-GCGATACCAAGAGGGACTTG-3′[f]
ML135	5′-CTTCTTATTCAAATGTAATAAAAGT-3′[e]

[a] Mutagenic primers used to introduce *Bam*HI (HH1) and *Hin*dIII (HH2) sites (underlined) around *BUD8* (see text).

[b] Primer used to introduce a *Not*I site (underlined) after the start codon of *BUD8* (see text).

[c] Primers used for deletion of *BUD9* (ΔBUD9-F and ΔBUD9-R) and for checking the success of the deletion construction (ΔBUD9-F and BUD9-R1) (see text). Primer BUD9-R1 corresponds to sequences ~150 bp downstream of the region deleted.

[d] Primers used to amplify the GFP coding sequence (see text). Primer GFP-F includes *Eco*RI and *Not*I sites (underlined) immediately upstream of sequences encoding the N-terminus of GFP. Primer GFP-R includes *Eco*RI, *Not*I, and *Bam*HI sites (underlined) immediately downstream of sequences encoding the C-terminus of GFP.

[e] Primers used to construct (LS10 and LS11) and check (LS8 and ML135) the chromosomal P_{GAL}-*GFP-BUD9* locus (see text).

[f] Primers used to introduce a *Not*I site just downstream of the *BUD9* start codon (see text). The *Not*I sites in primers LS34 and LS35 are underlined.

plac181, generating plasmid YEpGFP-BUD8. This plasmid also provided approximately normal Bud8p function (Figure 3D). The *Nco*I-*Bam*HI fragment (former site in the N-terminal portion of the GFP coding region, latter site introduced with primer GFP-R [Table 3]) was then replaced by the corresponding fragment from pKS-GFP*, generating plasmid YEpGFP*-BUD8.

To generate plasmids expressing tagged versions of Bud9p, the following strategy was used. First, using plasmid YCpBUD9 as template, two separate PCR reactions were conducted. One used forward primer LS33 (corresponding to vector sequences outside the polylinker and near the upstream end of the *BUD9*-containing insert) and reverse primer LS34 (corresponding to sequences overlapping the *BUD9* start codon and incorporating a *Not*I site just downstream of this start codon) (Table 3). The other used forward primer LS35 (corresponding to sequences overlapping the *BUD9* start codon and incorporating a *Not*I site just downstream of this start codon) and reverse primer LS36 (corresponding to sequences within the *BUD9* ORF). The products from these two reactions were digested with *Not*I and ligated together, and the resulting linear product was used as template in a second round of PCR using primers LS33 and LS36. The resulting product was digested with *Kpn*I (one site from the original vector polylinker, just outside the junction with the *BUD9* upstream sequences, and the other site in the 5′ part of the *BUD9* ORF) and ligated into *Kpn*I-digested YCp-BUD9. After sequencing the entire *Kpn*I segment to confirm the presence of the *Not*I site and the absence of mutations introduced by the PCR, *Not*I fragments containing triple-HA and GFP^{S65T} coding sequences (see above) were cloned into the *Not*I site, thus generating plasmids YCpHA-BUD9 and YCpGFP-BUD9. In addition, *Sph*I fragments from YCpHA-BUD9 and YCpGFP-BUD9 (one site near the upstream end of the *BUD9* upstream sequences; the other site from the vector polylinker) were subcloned into *Sph*I-digested YEplac195 to generate plasmids YEpHA-BUD9 and YEpGFP-BUD9, respectively. Diploid strains carrying YCpHA-BUD9 or YCpGFP-BUD9 as their sole source of Bud9p showed a partial restoration of Bud9p-dependent proximal-pole budding (Figure 3, E and G; cf. Figure 3M), and use of the proximal pole approached wild-type levels (Figure 3A) when YEpHA-BUD9 or YEpGFP-BUD9 provided the sole source of Bud9p (Figure 3, F and H). These data suggest that the tagged versions of Bud8p and Bud9p are partially, but not completely, functional.

To construct a strain expressing GFP-Bud9p at the *BUD9* chromosomal locus under P_{GAL} control, we used the PCR method (Longtine *et al*., 1998b). A fragment generated using plasmid pFA6a-His3MX6-PGAL1-GFP as template and primers LS10 and LS11 (Table 3) was transformed into strain YEF473, selecting for stable His^+ transformants, which should have P_{GAL} followed by GFP^{S65T} sequences fused in frame to *BUD9* sequences. Strain LSY42 was one such transformant. A PCR check using forward primer ML135 (corresponding to sequences within P_{GAL}) and reverse primer LS8 (corresponding to sequences downstream of the *BUD9* start codon) confirmed that *BUD9* had been modified as expected, and tetrad analysis showed that LSY42 was heterozygous for the modified and wild-type *BUD9* alleles. Two P_{GAL}-*GFP-BUD9* segregants from LSY42 were mated to produce strain LSY41. When grown on 2% raffinose, strain LSY41 displayed approximately normal levels of budding at the proximal pole (Figure 3I), consistent with the other evidence (see above) that GFP-tagged Bud9p is at least partially functional.

Analysis of Growth Rates and Mating Efficiencies

Growth rates in liquid medium were analyzed by growing cells to exponential phase, recording the OD_{660}, diluting the culture twofold with prewarmed medium, and determining the time required to grow back to the original OD_{660}. Growth on plates was analyzed by comparing colony sizes. Tests of sensitivity to Calcofluor and caf-

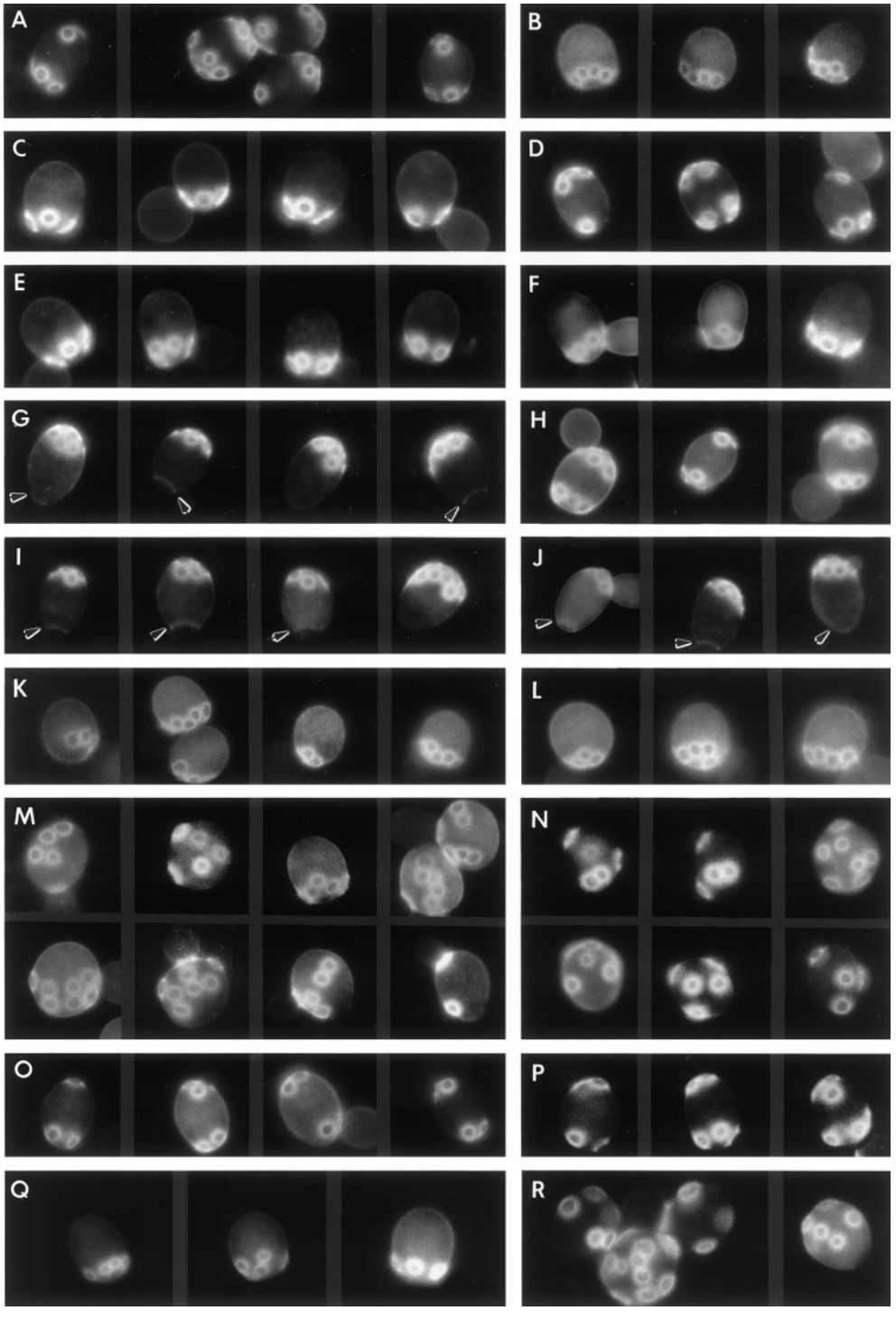

Figure 2. Budding-pattern phenotypes of wild-type and mutant strains, a strain overexpressing Bud8p, and strains expressing tagged versions of Bud8p. Cells of the indicated strains were stained with Calcofluor to visualize bud scars. (A–P) Cells growing exponentially in YM-P medium or medium selective for the indicated plasmid were examined. (A) Wild-type diploid strain YEF473; (B) wild-type haploid strain YEF473A; (C and D) *bud8-1/bud8-1* strain YHH274 containing no plasmid (C) or the low-copy *BUD8* plasmid YCpBUD8 (D); (E) *bud8-Δ1/bud8-Δ1* strain YHH415; (F) *bud8-Δ1/bud8–1* strain YHH399; (G and H) *bud9-1/bud9-1* strain YHH273 containing no plasmid (G) or the low-copy *BUD9* plasmid YCpBUD9 (H); (I) *bud9-Δ1/bud9-Δ1* strain YHH615; (J) *bud9-Δ1/bud9–1* strain YHH616; (K) Haploid *bud8-Δ1* strain YHH391; (L) Haploid *bud9-Δ1* strain YHH613; (M) *bud8-Δ1/bud8-Δ1 bud9-Δ1/bud9-Δ1* double-mutant strain YHH625; (N) *bud8-Δ1/bud8-Δ1 bud9-Δ1/bud9-Δ1 bud3Δ::HIS3/bud3Δ::HIS3* triple-mutant strain YHH772; (O) *bud8-Δ1/bud8-Δ1 URA3:HA-BUD8/URA3:HA-BUD8* strain YHH514; (P) *bud8-Δ1/bud8-Δ1 URA3:GFP-BUD8/URA3:GFP-BUD8* strain YHH529. (Q and R) *bud8-Δ1/bud8-Δ1* strain YHH415 carrying control plasmid YCpIF2 (Q) or plasmid YCpGAL-BUD8 (R) was grown overnight to exponential phase in SC-Leu medium containing 2% galactose instead of glucose to induce expression of P_{GAL}-*BUD8*. Arrowheads in G, I, and J indicate birth scars; these are difficult to see in the other panels because of the bud scars around the proximal poles.

feine were conducted as described previously (Ram *et al.*, 1994; Lussier *et al.*, 1997b). Mating efficiencies were analyzed by growing ***a*** and α strains to exponential phase in YM-P medium, collecting the cells on filters as described previously (Reid and Hartwell, 1977), incubating the filters on YPD plates for 3 h, removing the cells by vortexing in YM-P medium, sonicating for 2 s, and counting the numbers of zygotes.

Protein Analyses

Protein Extraction. Yeast cells were grown at 30°C in SC medium lacking particular nutrients as needed for selection of various plasmids. Total cell lysates were prepared from late-exponential-phase cultures (OD_{600} of ≈3.0) essentially as described by Ljungdahl *et al.* (1992). Briefly, cells were harvested by centrifugation at 23°C,

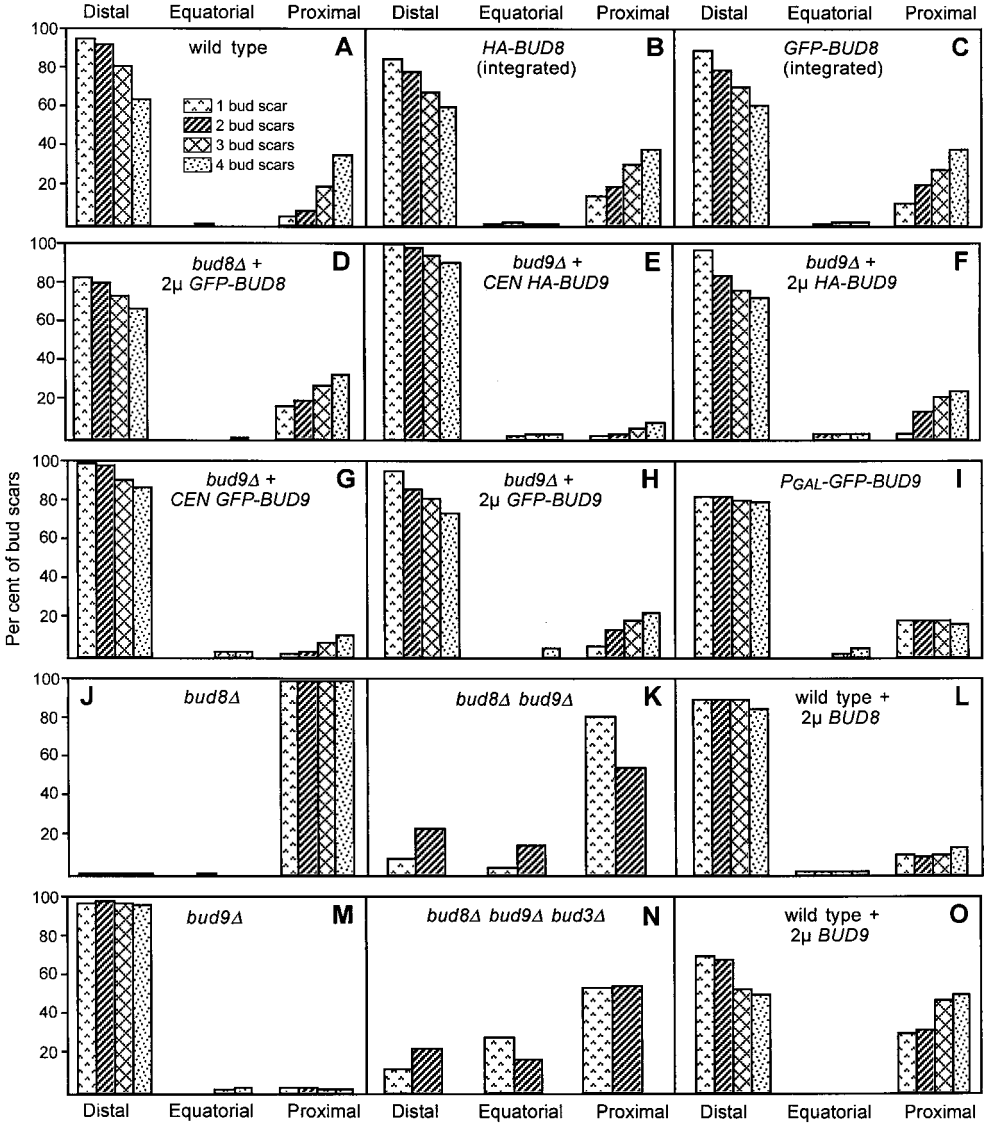

Figure 3. Quantitative evaluation of bud position in wild-type and mutant strains, strains overexpressing Bud8p or Bud9p, and strains expressing tagged versions of Bud8p or Bud9p. Cells of the indicated strains were grown and stained as described in the legend to Figure 2, A–P, except that strain LSY41 was grown with 2% raffinose instead of 2% glucose as carbon source. For each experiment, the positions of all bud scars were determined for 100 cells with one bud scar, 100 cells with two bud scars, 100 cells with three bud scars, and 100 cells with four bud scars. (Thus, for each experiment, the "1 bud scar" bars represent 100 total bud scars, the "2 bud scars" bars represent 200 total bud scars, etc.) The positions of bud scars were scored as distal pole (the third of the cell most distal to the birth scar), equatorial (the middle third of the cell), or proximal pole (the third of the cell centered on the birth scar). In each panel, the average values from three independent experiments are shown. (A) Wild-type strain YEF473; (B) *bud8-Δ1/bud8-Δ1 URA3:HA-BUD8/URA3:HA-BUD8* strain YHH514; (C) *bud8-Δ1/bud8-Δ1 URA3:GFP-BUD8/URA3:GFP-BUD8* strain YHH529; (D) *bud8-Δ1/bud8-Δ1* strain YHH415 carrying the high-copy *GFP-BUD8* plasmid YEpGFP-BUD8; (E–H) *bud9-Δ1/bud9-Δ1* strain YHH615 carrying plasmid YCpHA-BUD9 (E), YEpHA-BUD9 (F), YCpGFP-BUD9 (G), or YEpGFP-BUD9 (H); (I) P_{GAL}*-GFP-BUD9/*P_{GAL}*-GFP-BUD9* strain LSY41; (J) *bud8-Δ1/bud8-Δ1* strain YHH415; (K) *bud8-Δ1/bud8-Δ1 bud9-Δ1/bud9-Δ1* strain YHH625; (L) strain YEF473 carrying the high-copy *BUD8* plasmid YEpBUD8; (M) *bud9-Δ1/bud9-Δ1* strain YHH615; (N) *bud8-Δ1/bud8-Δ1 bud9-Δ1/bud9-Δ1 bud3Δ::HIS3/bud3Δ::HIS31* strain YHH772; (O) strain YEF473 carrying the high-copy *BUD9* plasmid YEpBUD9.

washed once with lysis buffer (10 mM Tris-HCl, pH 7.5, 5 mM $MgCl_2$, 100 mM NaCl, 300 mM sorbitol, plus one protease inhibitor cocktail tablet [Roche Molecular Biochemicals] per 25 ml [i.e., twice the normal dosage]), and resuspended in lysis buffer to an OD_{600} of ≈50. The cells were then broken by six cycles of vortexing for 30 s with glass beads interspersed with 30-s periods of cooling in an ice bath. The crude lysate was centrifuged at 1600 rpm (200 × *g*) for 5 min to remove nonlysed cells, and the supernatant was collected as the total cell lysate and stored at −80°C.

Electrophoresis and Immunoblotting. Samples were diluted fivefold with 5×-concentrated sample buffer (Laemmli, 1970), heated at 100°C for 5 min, and subjected to SDS-PAGE using 8% gels (Laemmli, 1970). For immunoblotting, proteins were transferred to nitrocellulose membranes (Schleicher & Schuell, Keene, NH) by electrophoresis overnight at 30 V in a Bio-Rad (Hercules, CA) Mini-Protean II apparatus. The membranes were blocked for 1 h at 23°C in TBST buffer (10 mM Tris-HCl, pH 8.0, 150 mM NaCl, 0.05% Tween 20) containing 5% nonfat dry milk powder and then incubated for 1 h at 23°C in the same buffer containing anti-HA monoclonal antibody 12CA5 (Roche Molecular Biochemicals; used at a 1:2000 dilution), an anti-invertase polyclonal antiserum (Lussier *et al.*, 1996; used at a 1:1000 dilution), or affinity-purified anti-Bud8p antibodies (see below; used at a 1:100 dilution). The membranes were then washed in TBST buffer and incubated for 1 h at 23°C in TBST buffer containing 5% nonfat dry milk powder and a 1:2000 dilution of horseradish peroxidase-conjugated sheep anti-mouse-IgG or donkey anti-rabbit-IgG secondary antibody (Amersham Pharmacia Biotech, Piscataway, NJ), as appropriate. The blots were then washed further with TBST, and proteins were visualized using the enhanced chemiluminescence Western-blotting detection reagents (Amersham Pharmacia Biotech) according to the manufacturer's instructions.

Analysis of Membrane Association. To 80 μl of total cell lysate were added 20 μl of lysis buffer (as control), 0.5 M Na_2CO_3 (pH 11), 3 M NaCl, 8 M urea, 20% Triton X-100, or 10.0% SDS. These samples were incubated for 20 min on ice (or at 23°C for the Triton and SDS samples) and then centrifuged for 1 h at 100,000 × *g* to separate the insoluble membrane materials in the pellet from the soluble materials in the supernatant. These fractions were then analyzed by SDS-PAGE and immunoblotting. Alternatively, to test for possible plasma membrane association (Goud *et al.*, 1988), an aliquot of total cell extract was centrifuged for 5 min at 10,000 × *g* at 4°C, and the supernatant and pellet fractions were analyzed separately by SDS-PAGE and immunoblotting.

Analysis of Protein Glycosylation. Possible *O*-linked glycosylation was investigated by analyzing proteins from appropriate mutant strains (see RESULTS). Possible *N*-linked glycosylation was investigated by analyzing proteins from appropriate mutant strains (see RESULTS) and/or by digestion of proteins in total cell lysates either with a recombinant endo-β-*N*-acetylglucosaminidase H/maltose-binding-protein fusion protein ($EndoH_f$; New England Biolabs) or with a mixture of endoglycosidase F and peptide-*N*-glycosidase F (EndoF/PNGaseF; Oxford GlycoSciences, Bedford, MA). $EndoH_f$ was used essentially as described by the manufacturer (see also Roemer *et al.*, 1994). For EndoF/PNGaseF digestion, several microliters of total cell lysate were mixed with water and a denaturation buffer cocktail to give a total volume of 12.5 μl at final concentrations of 20 mM sodium phosphate, pH 7.5, 55 mM EDTA, 0.075% SDS, 0.5% β-mercaptoethanol, 2 μM phenylmethylsulfonyl fluoride, 1 μg/ml leupeptin, and 1 μg/ml pepstatin. This mixture was heated to 100°C for 10 min and then cooled to 23°C. To counteract the inhibition of PNGaseF by SDS, 5.5 μl of an octylglycoside preparation (1.82% octylglycoside in 20 mM sodium phosphate, pH 7.5, 55 mM EDTA, plus protease inhibitors as described above) was added, followed by 2.0 μl of the EndoF/PNGaseF preparation (in 20 mM potassium phosphate, pH 7.2, 50 mM EDTA), giving a final enzyme concentration of 340 deglycosylation units/ml. After incubation overnight at 37°C, samples were analyzed by SDS-PAGE and immunoblotting as described above. In these experiments, controls were mock-digested by being subjected to identical treatment but without the deglycosylation enzymes.

Generation of Antibodies to Bud8p

To generate fusions of *E. coli* maltose-binding protein (MBP) and TrpE to Bud8p, the *BUD8*-containing *Bam*HI-*Hin*dIII fragment from pALT-BUD8(B/H) (see above) was subcloned into the corresponding sites of pMAL-c2 (New England Biolabs) and pATH3 (Koerner *et al.*, 1991) to generate plasmids pMAL-BUD8 and pATH-BUD8. Sequencing across the junctions confirmed that in-frame fusions had been constructed. When *E. coli* DH5α cells containing these plasmids were induced by standard procedures (Ausubel *et al.*, 1995), only extensively degraded proteins were observed by SDS-PAGE (our unpublished results). Thus, shorter fusion genes (containing 877 bp of *BUD8* coding sequence; Figure 1A) were generated by digesting pMAL-BUD8 and pATH-BUD8 with *Sal*I and *Hin*dIII, blunting the ends with Klenow-fragment polymerase, and religating. Induction of these genes in *E. coli* DH5α cells and analysis by SDS-PAGE revealed primarily undegraded fusion proteins of the expected sizes of 72 kDa (MBP-Bud8pSal) and 70 kDa (TrpE-Bud8pSal) (our unpublished results). MBP-Bud8pSal was purified on an amylose-agarose column (New England Biolabs) as described previously (Ausubel *et al.*, 1995) and used to raise polyclonal rabbit antisera by standard procedures (Cocalico Biologicals, Reamstown, PA). Antisera were tested by immunoblotting against TrpE-Bud8pSal. Antibodies from a serum obtained after four booster injections were affinity purified first against TrpE-Bud8pSal and then against MBP-Bud8pSal, using nitrocellulose strips containing the fusion proteins (Pringle *et al.*, 1991). The purified antibodies were concentrated using a Centricon-3 filter (Amicon, Danvers, MA), and bovine serum albumin (BSA) was added to 0.1%.

When tested by immunoblotting (see above), the purified antibodies recognized two polypeptides, with apparent molecular weights of ~120 and ~74 kDa, in extracts of cells carrying a high-copy *HA-BUD8* plasmid (our unpublished results). Because the ~120-kDa species was not detected in extracts of cells carrying a control plasmid, it appears to represent Bud8p, consistent with the results obtained with the use of HA-specific antibodies (Figures 5–7, below). In immunofluorescence experiments, the purified antibodies yielded a signal in *bud8*Δ cells that were overexpressing Bud8p from the *GAL* promoter (Figure 8C). Because this signal was not detected in wild-type cells or in *bud8*Δ cells containing the control plasmid YCpIF2 (our unpublished results), it appears to be specific for Bud8p.

Staining and Microscopy

For characterization of budding patterns, cells were generally fixed with 3.7% formaldehyde and stained with 0.1–1 mg/ml Calcofluor as described by Pringle *et al.* (1989). For some counts and for simultaneous visualization of a GFP signal together with birth and bud scars, unfixed cells were stained with 1 μg/ml Calcofluor as described by Zahner *et al.* (1996). Cells were examined and photographed on a Nikon Microphot SA microscope using an Apo 60X/1.40 NA oil-immersion objective and Kodak T-Max 400 film.

Living cells expressing GFP-Bud8p or GFP-Bud9p were observed either by conventional fluorescence microscopy (as just described) using the fluorescein isothiocyanate filter set or by time-lapse digital-imaging microscopy. The time-lapse experiments were performed essentially as described by Salmon *et al.* (1998). Cells were grown overnight in minimal medium plus casamino acids and observed in the same medium containing 25% gelatin. Observations were made using a Nikon Microphot FXA microscope equipped with a Hamamatsu charge-coupled device camera and an Apo 60X/1.4 NA oil-immersion objective. Images were collected at 1-min intervals using 3-s exposures and analyzed using Metamorph software (Universal Imaging, West Chester, PA).

Cells to be used for immunofluorescence were fixed by adding formaldehyde directly to the growth medium to a final concentration of 3.7% and swirling gently for 1.5 h at 23°C. Localization of Cdc11p and of tubulin was performed essentially as described previously (Pringle *et al.*, 1991) using a rabbit polyclonal anti-Cdc11p (Ford and Pringle, 1991) and the YOL1/34 rat monoclonal anti-tubulin (Kilmartin and Adams, 1984; obtained from Accurate Chemical and Scientific, Westbury, NY). The secondary antibodies were Cy2-conjugated goat anti-rabbit-IgG and rhodamine-conjugated goat anti-rat-IgG (both from Jackson Immunoresearch, West Grove, PA). For immunolocalization of Bud8p, the fixed cells were washed once in phosphate-buffered saline (PBS) and once in solution A (40 mM potassium phosphate, pH 6.5, 0.5 mM $MgCl_2$, 1.2 M sorbitol [Pringle *et al.*, 1991]), followed by treatment with 1% β-mercaptoethanol and 0.5 mg/ml lyticase (catalog no. 152270; ICN Biomedicals, Costa Mesa, CA) in solution A for 40 min at 37°C to remove cell walls. The cells were then washed twice with solution A and once with PBS, resuspended in PBS containing 1% BSA (PBS/BSA), and applied to polylysine-coated slides as described previously (Pringle *et al.*, 1991). Affinity-purified anti-Bud8p antibody diluted 1:10 in PBS/BSA was then applied, and the slide was incubated for 1 h at 23°C. After washing with PBS/BSA, the cells were incubated for 1 h at 23°C in BODIPY-FL-conjugated goat anti-rabbit-IgG antibody (Molecular Probes) diluted 1:200 in PBS/BSA. The cells were then washed further with PBS/BSA and mounted as described previously (Pringle *et al.*, 1991).

RESULTS

Cloning of BUD8 *and* BUD9

To clone *BUD8* and *BUD9,* we transformed *bud8* and *bud9* mutant diploid strains with a yeast genomic-DNA library in

a low-copy vector and examined individual transformants by fluorescence microscopy for restoration of the bipolar budding pattern (see MATERIALS AND METHODS). Subcloning localized the *bud8*-complementing activity to an ~3.0-kb *Bam*HI-*Xba*I fragment (Figures 1A and 2, C and D). This fragment hybridized to a λ′ clone carrying DNA from chromosome arm XIIR between *ILV5* and *CDC3,* very close to the map location of *bud8-1* (Zahner *et al.*, 1996). Sequencing of the *Bam*HI-*Sca*I fragment (Figure 1A; accession no. L37016) revealed one complete and one partial ORF. Subsequent release of chromosome XII sequence by the genome project (accession no. U19102) identified the complete ORF as *YLR353W* and the adjacent incomplete ORF as *YLR354C* (*TAL1*). A diploid strain homozygous for a deletion of *YLR353W* (Figure 1A; see MATERIALS AND METHODS) budded only from the proximal pole (Figure 2E), like the original *bud8-1* mutant (Figure 2C), and the *Bam*HI-*Xba*I fragment on a low-copy plasmid restored bipolar budding (our unpublished results). In addition, the deletion failed to complement *bud8-1* (Figure 2F). The similar phenotypes, noncomplementation, and coincidence in map position establish that *YLR353W* is *BUD8.*

Subcloning localized the *bud9*-complementing activity to an ~2.7-kb *Nsi*I fragment (Figures 1B and 2, G and H). This fragment hybridized to λ′ clones carrying DNA from chromosome arm VIIR between *KSS1* and *RME1*, very close to the map position of *bud9-1* (Zahner *et al.*, 1996). The *Nsi*I fragment was sequenced (accession no. AF302239) and found to contain a single ORF. Comparison of our sequence to that from the genome project (accession no. Z72826) identified this ORF as *YGR041W.* A diploid strain homozygous for a deletion of *YGR041W* (Figure 1B; see MATERIALS AND METHODS) budded only from the distal pole (Figure 2I), like the original *bud9-1* mutant (Figure 2G), and the *Nsi*I fragment on a low-copy plasmid restored bipolar budding (our unpublished results). In addition, the deletion failed to complement *bud9-1* (Figure 2J). The similar phenotypes, noncomplementation, and coincidence in map position establish that *YGR041W* is *BUD9.*

Deletion and Overexpression Phenotypes of BUD8 *and* BUD9

As noted above, diploid strains homozygous for the *bud8-*Δ*1* and *bud9-*Δ*1* deletions resembled the original *bud8-1* and *bud9-1* mutants in budding pattern. However, quantitative analysis showed that the deletion phenotypes were somewhat more extreme, at least in the case of *BUD8.* Although *bud8-1* cells produce a few buds at their distal poles (Zahner *et al.*, 1996), *bud8-*Δ*1* cells budded almost exclusively at their proximal poles through their first four cell cycles (Figure 3J). Similarly, *bud9-*Δ*1* cells budded almost exclusively from their distal poles (Figure 3M). Like *bud8-1* and *bud9-1* (Zahner *et al.*, 1996), the *bud8-*Δ*1* and *bud9-*Δ*1* mutations had no detectable effects on axial budding (Figure 2, K and L). However, it should also be noted that the bud scars at the proximal pole in diploid *bud8* mutants form clusters such as those seen on bipolar-budding cells rather than the single chains found on axially budding cells (compare Figure 2, C and E, to B, K, and L).

The *bud8-*Δ*1* and *bud9-*Δ*1* strains were also examined for other possible phenotypes. However, no significant differences from wild type were found in growth rates on liquid or solid, rich or defined medium over a range of temperatures (our unpublished results), in overall cell morphology (Figure 2), or in the mating efficiencies of haploid strains (crosses of strains YHH391 by YHH394, YHH613 by YHH614, and YEF473A by YEF473B were compared as described in MATERIALS AND METHODS). In addition, the *bud8-*Δ*1* and *bud9-*Δ*1* strains did not differ significantly from wild type in their sensitivities to Calcofluor or caffeine (our unpublished results), suggesting that Bud8p and Bud9p do not play major structural roles in the cell wall and that the altered sensitivities to these drugs observed previously for a *bud8* mutant (Lussier *et al.*, 1997b) were specific to the particular mutation and/or strain examined.

The loss of distal-pole budding in *bud8* mutant strains and of proximal-pole budding in *bud9* mutant strains suggests that Bud8p and Bud9p may mark the distal and proximal poles, respectively, for bipolar budding. In this case, it might be expected that a *bud8-*Δ*1 bud9-*Δ*1* double-mutant diploid strain would bud at random sites. Indeed, such a strain showed a partially randomized budding pattern (Figure 2M). However, the occurrence of some apparent chains of bud scars (Figure 2M) and a tendency to bud at the proximal pole (Figure 3K) suggested that under these conditions (i.e., the putative absence of both types of bipolar-budding markers), a diploid strain might show some ability to use axial cues for bud-site selection. Indeed, when Bud3p (a component of the axial site-selection machinery [Chant *et al.*, 1995]) was also absent, a more fully randomized pattern of budding was observed (Figures 2N and 3N).

If Bud8p and Bud9p are really markers for bipolar budding, it might be predicted that overproduction of one of these proteins would either enhance the use of the marked pole for budding or randomize bud position (by producing a delocalized signal). Indeed, both effects could be observed. When *BUD8* was expressed from its own promoter on a high-copy plasmid, the cells showed a more persistent bias for the use of the distal pole (Figure 3L), whereas the presence of a high-copy *BUD9* plasmid resulted in increased use of the proximal pole during the first few cell cycles (Figure 3O). (Strikingly, although cells whose first four buds were all at the proximal pole were very rare in wild-type strains [Chant and Pringle, 1995], 9% of the cells were of this type in the population shown in Figure 3O.) In contrast, when *BUD8* was expressed (presumably to high levels) from the *GAL* promoter, bud-site positions were largely random (Figure 2, Q and R).

Analysis of Bud8p and Bud9p Sequences

The predicted sequences of Bud8p and Bud9p revealed that the two proteins are very similar in overall structure despite a modest difference in length (Figure 4). Each protein has a long, hydrophilic N-terminal domain followed by two short hydrophobic domains surrounding a short hydrophilic domain. The program TM-pred (Hofmann and Stoffel, 1993) predicts that each of the hydrophobic domains is membrane-spanning and that the N-terminal domain of each protein is in the extracytoplasmic space despite the absence of N-terminal signal sequences. This prediction is consistent with the presence of multiple potential sites for *N*-linked glycosylation within each N-terminal domain and with their high serine + threonine content (suggestive of possible *O*-linked glycosylation [Orlean, 1997]). Although there is little

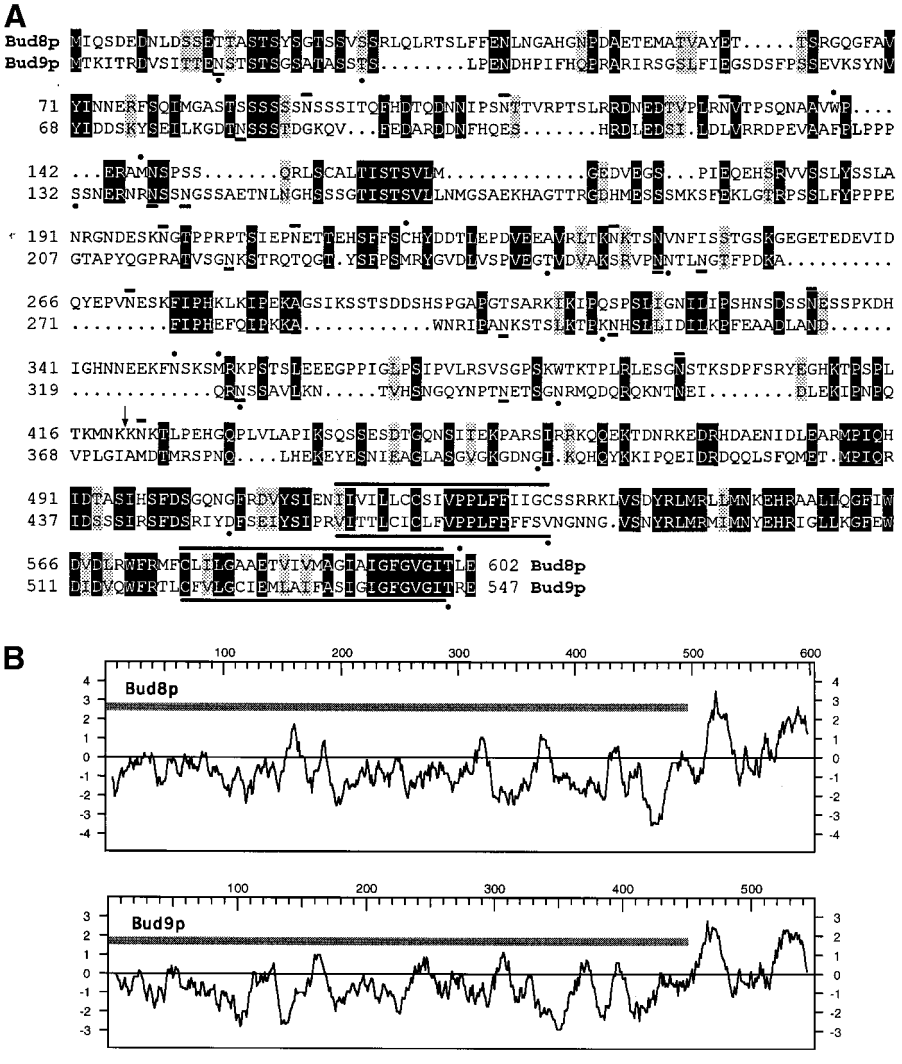

Figure 4. Analysis of the Bud8p and Bud9p sequences. (A) Sequences of Bud8p and Bud9p were aligned with the use of the GCG GAP Program. Black shading, identical amino acids; gray shading, similar amino acids (I, L, V; D, E; N, Q; K, R; S, T); small dots, gaps introduced to maximize sequence alignment; long overlines and underlines, hydrophobic putative transmembrane domains (see text and B); short overlines and underlines, possible sites of *N*-linked glycosylation (Asn – X – Ser/Thr, where X is any amino acid but Pro); arrow, site at which the genome-project sequence for *BUD8* indicates three nucleotides (AAG; amino acid K) that are not present in our sequence; large dots, sites at which the genome-project sequences predict amino acids different from those predicted by our sequences (see MATERIALS AND METHODS for details). (B) Hydropathy analysis of Bud8p and Bud9p with the use of the program of Kyte and Doolittle (1982) with a window size of 11. Shaded bars, regions that are Ser/Thr rich (24% Ser + Thr for Bud8p; 21% Ser + Thr for Bud9p) and contain all of the potential sites for *N*-linked glycosylation.

similarity in sequence between the N-terminal portions of the proteins, there is strong similarity (53% sequence identity) between their C-terminal 116 amino acids (Figure 4A). Interestingly, the regions with sequence similarity include the predicted transmembrane domains (including the two conserved prolines in the upstream domains) and the ~30 amino acids just N-terminal to them, as well as the predicted cytoplasmic loops. Surprisingly, Bud9p does not share the cluster of positively charged amino acids found just C-terminal to the first predicted transmembrane domain in Bud8p, which might have been thought to be critical in determining the orientation of insertion of this domain into the endoplasmic reticulum membrane (Hartmann *et al.*, 1989; von Heijne, 1996; Sääf *et al.*, 1999). To date, no homologs of Bud8p or Bud9p from other organisms have appeared in the databases.

Membrane Association and Glycosylation of Bud8p and Bud9p

To test the membrane association and topology predicted from the Bud8p and Bud9p sequences, we carried out fractionation experiments and tests of glycosylation using strains expressing functional HA-epitope-tagged versions of the proteins. Although expression of HA-Bud8p from a low-copy plasmid (YCpHA-BUD8) resulted in only a faint signal upon immunoblotting with the anti-HA antibody (our unpublished results), a somewhat fuzzy band was visualized clearly when a high-copy plasmid was used (Figure 5A, lane 2). This band was not seen in control extracts (Figure 5A, lane 1) and corresponded to a polypeptide of apparent molecular weight ~121 kDa, much larger than the ~69 kDa predicted from the Bud8p and HA sequences. On fractionation in lysis buffer or in the presence of Na_2CO_3, NaCl, urea, or Triton X-100, this polypeptide remained in the pellet fraction (Figure 5A, lanes 3–12), but it was extracted into the supernatant upon treatment with SDS (Figure 5A, lanes 13–14). Essentially identical results were obtained with HA-Bud9p, except that in this case the signal was observed clearly even when a low-copy plasmid was used (Figure 5B). HA-Bud9p had an apparent molecular weight of ~110 kDa, much larger than the ~64 kDa predicted from the Bud9p and HA sequences. Because treatment with NaCl or urea should release most peripheral membrane proteins and

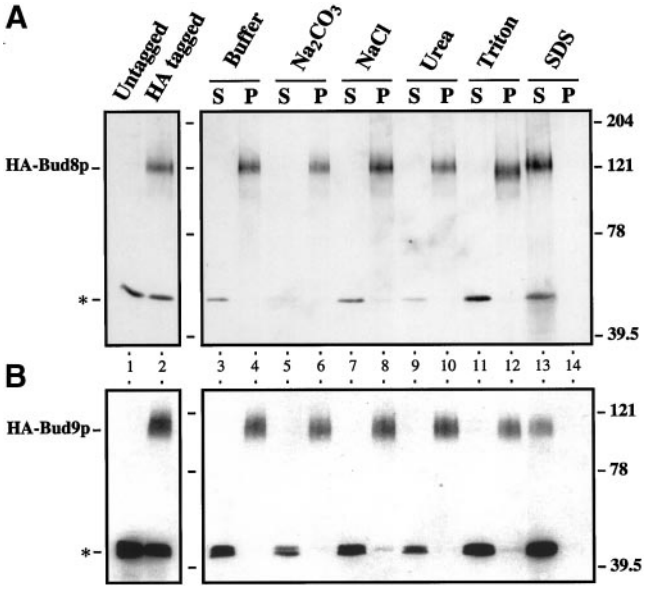

Figure 5. Membrane association of Bud8p and Bud9p. (A) Total cell lysates were prepared as described in MATERIALS AND METHODS from strain YHH415 containing a high-copy plasmid expressing untagged Bud8p (YEpBUD8-6, lane 1) or a similar plasmid expressing HA-Bud8p (YEpHA-BUD8-6, lanes 2–14). Untreated (lanes 1 and 2) and treated (lanes 3–14) lysates were analyzed by SDS-PAGE and immunoblotting with the anti-HA antibody. Samples of lysate were treated with lysis buffer (lanes 3 and 4), 0.1 M Na_2CO_3 (lanes 5 and 6), 0.6 M NaCl (lanes 7 and 8), 1.6 M urea (lanes 9 and 10), 4% Triton X-100 (lanes 11 and 12), or 2% SDS (lanes 13 and 14) and centrifuged to separate supernatant (S) and pellet (P) fractions as described in MATERIALS AND METHODS. (B) Total cell lysates were prepared from strain SEY6210D containing a low-copy plasmid expressing untagged Bud9p (YCpBUD9, lane 1) or a similar plasmid expressing HA-Bud9p (YCpHA-BUD9, lanes 2–14) and analyzed as described for A. An endogenous protein recognized by the anti-HA antibody is indicated by an asterisk. The presence of this protein almost exclusively in the supernatant fractions (lanes 3–14) indicates that the pellet fractions were largely free of contamination by soluble proteins. Molecular size standards (in kDa) are indicated on the right.

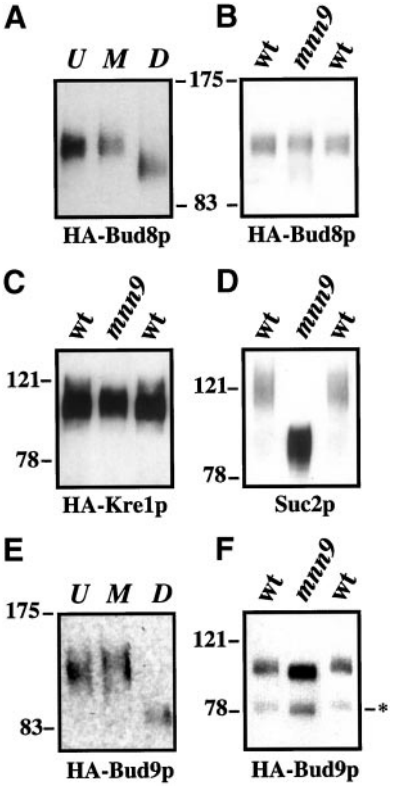

Figure 6. *N*-linked glycosylation of Bud8p and Bud9p. (A and E) Total cell lysates were prepared as described in MATERIALS AND METHODS from strain YHH415 containing the high-copy *HA-BUD8* plasmid YEpHA-BUD8–6 (A) and from strain SEY6210D containing the low-copy *HA-BUD9* plasmid YCpHA-BUD9 (E). After no further treatment (U), mock digestion (M), or digestion with an Endo F/PNGase mixture (see MATERIALS AND METHODS), samples were analyzed by SDS-PAGE and immunoblotting with the anti-HA antibody. (B–D and F) Total cell lysates were prepared from wild-type strain SEY6210 (wt) and *mnn9* deletion strain HAB880 (*mnn9*) containing the high-copy *HA-BUD8* plasmid YEpHA-BUD8-6 (B), the high-copy *HA-KRE1* plasmid CB612-Kre1p-HA (C), the high-copy *SUC2* plasmid Yep352-SUC2 (D), or the high-copy *HA-BUD9* plasmid YEpHA-BUD9 (F). After SDS-PAGE, proteins were detected with the use of the anti-HA antibody (B, C, and F) or anti-invertase antibody (D) (see MATERIALS AND METHODS). In F, the asterisk indicates a possible degradation product that was not seen in other experiments with HA-Bud9p. For each panel, molecular weight standards (in kDa) are indicated.

treatment with Na_2CO_3 should release soluble proteins from membrane vesicles (Fujiki *et al.*, 1982; Goud *et al.*, 1988; Ljungdahl *et al.*, 1992; Roemer *et al.*, 1994, 1996a), the data suggest that Bud8p and Bud9p are indeed integral membrane proteins. When an extract of cells expressing HA-Bud8p was centrifuged at 10,000 × *g* (see MATERIALS AND METHODS), most Bud8p was found in the pellet (our unpublished results), suggesting that most Bud8p was in the plasma membrane (Goud *et al.*, 1988).

It seemed likely that the high apparent molecular weights of Bud8p and Bud9p reflected glycosylation of the proteins. To test for possible *N*-linked glycosylation, we treated cell extracts with enzymes that remove *N*-linked glycosyl side chains. For both HA-Bud8p and HA-Bud9p, treatment either with an Endo F/PNGase mixture (Figure 6, A and E) or with Endo H (our unpublished results) led to a substantial decrease in apparent molecular weight, although both proteins still migrated considerably more slowly than expected from the sizes of their polypeptide chains. Because all of the potential sites for *N*-linked glycosylation are in the N-terminal domains of the proteins (Figure 4A), this evidence for *N*-linked glycosylation strongly supports the hypothesis that the N-terminal domains are in the extracytoplasmic space.

To characterize the *N*-linked glycosylation further, HA-Bud8p and HA-Bud9p were expressed in a strain lacking Mnn9p, which is required for the elaboration of *N*-glycan outer chains (Yip *et al.*, 1994; Orlean, 1997; Shahinian *et al.*, 1998). As controls, an HA-tagged Kre1p (which is heavily *O*-glycosylated but not *N*-glycosylated [Boone *et al.*, 1990; Roemer and Bussey, 1995]) and Suc2p (which is both *O*- and *N*-glycoslyated, with highly elaborated *N*-glycosyl outer chains [Esmon *et al.*, 1987; Reddy *et al.*, 1988]) were ex-

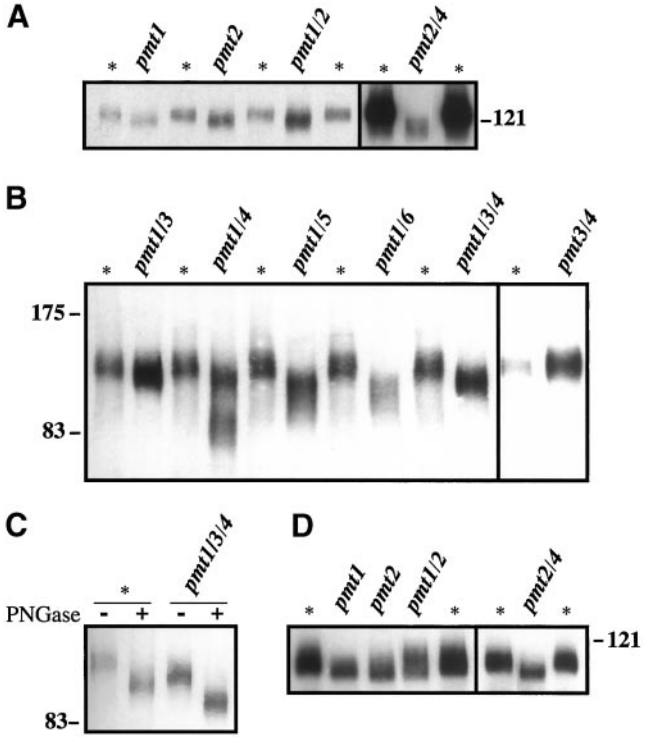

Figure 7. *O*-linked glycosylation of Bud8p and Bud9p. Total cell lysates were prepared from the indicated strains as described in MATERIALS AND METHODS and analyzed by SDS-PAGE and immunoblotting with the anti-HA antibody. Strains used were wild type, SEY6210 (lanes indicated by *); *pmt1,* HAB897; *pmt2,* HAB898; *pmt1 pmt2,* HAB899; *pmt2 pmt4,* Pmt2/4; *pmt1 pmt3,* Pmt1/3; *pmt1 pmt4,* Pmt1/4; *pmt1 pmt5,* Pmt1/5; *pmt1 pmt6,* Pmt1/6; *pmt1 pmt3 pmt4,* Pmt1/3/4; *pmt3 pmt4,* Pmt3/4. (A–C) All strains carried a high-copy *HA-BUD8* plasmid, either YEpHA-BUD8–6 (A and the right-hand two lanes in B) or YEpHA-BUD8–5 (C and the other lanes in B). For C, extracts were either mock-digested (−) or digested with an Endo F/PNGase mixture (+; see MATERIALS AND METHODS and Figure 6) before SDS-PAGE. (D) All strains carried plasmid YEpHA-BUD9. In A, the two boxes show the results from independent immunoblots; in B and in D, the pairs of boxes show different parts of the same immunoblot, exposed for different times. For each panel, molecular weight standards (in kDa) are indicated.

pressed in the same *mnn9* mutant strain. As expected, HA-Kre1p from the *mnn9* and wild-type strains showed no difference in electrophoretic mobility (Figure 6C), whereas Suc2p migrated much more rapidly when expressed in the *mnn9* strain (Figure 6D). Surprisingly, HA-Bud8p from the *mnn9* and wild-type strains showed no detectable difference in mobility (Figure 6B), whereas HA-Bud9p from the *mnn9* strain showed only a small increase in mobility (Figure 6F). HA-Bud8p also showed no increase in mobility when expressed in strain HAB881, which is deficient in Och1p, the α-1,6-mannosyltransferase required for the initiation of outer chain formation (Nakayama *et al.*, 1992; Orlean, 1997; Shahinian *et al.*, 1998) (our unpublished results). Thus, it appears that most or all of the *N*-linked glycosyl chains on Bud8p and Bud9p consist of core units only, without elaborated outer chains.

To test for possible *O*-linked glycosylation, HA-Bud8p and HA-Bud9p were expressed in strains lacking one or more of the protein *O*-mannosyltransferase (Pmt) enzymes, which transfer the initial mannosyl residue from dolichyl-P-mannose to serine or threonine residues in the polypeptide (Tanner and Lehle, 1987; Gentzsch and Tanner, 1996, 1997; Orlean, 1997). When expressed in *pmt1*, *pmt2*, *pmt3*, *pmt4*, *pmt5*, or *pmt6* single-mutant strains, HA-Bud8p and HA-Bud9p showed slightly increased (Figure 7, A and D) or essentially the same (our unpublished results) mobilities relative to the proteins from wild-type cells. Expression of the proteins in strains carrying certain combinations of *pmt* mutations led to larger increases in mobility (Figure 7, A, B, and D), although for HA-Bud9p, even the largest increase in mobility observed (Figure 7D, *pmt2/4*) was rather modest. As expected, enzymatic removal of *N*-glycosyl chains from HA-Bud8p extracted from a *pmt* mutant strain led to a further increase in mobility (Figure 7C). Interestingly, however, the protein still migrated significantly more slowly than predicted from the size of its polypeptide chain (see DISCUSSION).

Localization of Bud8p and Bud9p in Wild-Type Cells

Previous analyses of bipolar budding had suggested that the distal-pole marker would arrive at the presumptive bud site before bud emergence and remain at the tip of the bud as the bud grew, thus eventually marking the distal pole of the daughter cell (Chant and Pringle, 1995; Amberg *et al.*, 1997). These analyses also suggested that the proximal-pole marker would arrive at the mother-bud neck shortly before cell division and remain in place during division, thus marking the proximal pole of the daughter cell. To ask whether Bud8p and Bud9p behaved as predicted for the distal-pole and proximal-pole markers, we localized these proteins with the use of an antibody specific for Bud8p and GFP-tagged fusion proteins that were at least partially functional (see MATERIALS AND METHODS).

In a strain carrying a chromosomal copy of *GFP-BUD8,* only ~10% of the cells showed any detectable GFP signal. Among such cells, GFP-Bud8p was observed in patches at presumptive bud sites on unbudded cells (Figure 8A, cells 1–3) and at the tips of buds of various sizes (Figure 8A, cells 4–6). Most of the unbudded cells had a single patch of GFP-Bud8p (Figure 8A, cell 1), but some had patches of GFP-Bud8p at both poles (Figure 8A, cells 2 and 3). When *GFP-BUD8* was expressed from a high-copy plasmid, the GFP signal was observed in a higher proportion (20–25%) of the cells and was typically somewhat brighter, but the patterns observed were very similar (Figure 8B; see also Figure 10A). In this case, however, most unbudded cells with a detectable signal had patches of GFP-Bud8p at both poles. When immunofluorescence was performed on wild-type cells using the affinity-purified anti-Bud8p antibodies, no signal was observed. However, when cells expressing *BUD8* under control of the *GAL* promoter were induced for several hours and then examined, patterns of Bud8p staining were observed that were essentially the same as those observed with GFP-tagged Bud8p (Figure 8C). Taken together, the results support the hypothesis that Bud8p is a component of the distal-pole marker, although the observation of unbudded cells with Bud8p at both poles is surprising.

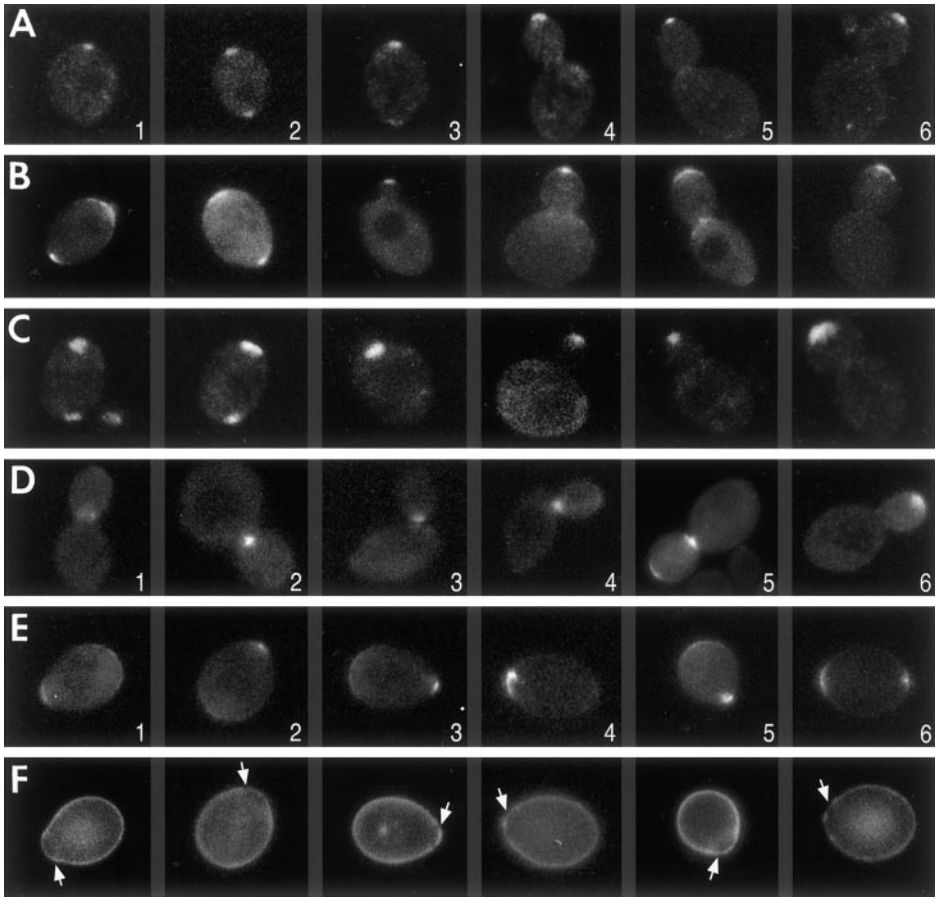

Figure 8. Localization of Bud8p and Bud9p with the use of GFP-tagged proteins (A, B, D, and E) or immunofluorescence with Bud8p-specific antibodies (C). Cells were observed by conventional fluorescence microscopy as described in MATERIALS AND METHODS. (A) Cells of strain YHH529 (*bud8-Δ1/bud8-Δ1 URA3:GFP-BUD8/URA3:GFP-BUD8*) were grown overnight on a YPD plate, then suspended in water for viewing. (B) Cells of *bud8-Δ1/bud8-Δ1* strain YHH415 carrying plasmid YEpGFP-BUD8 were grown overnight on an SC-Leu plate, then suspended in water for viewing. (C) Cells of strain YHH415 carrying plasmid YCpGAL-BUD8 were grown to exponential phase in SC-Leu medium containing 2% raffinose, shifted to SC-Leu medium containing 2% galactose for 4 h to induce expression of *BUD8,* and prepared for immunofluorescence as described in MATERIALS AND METHODS. (D–F) Cells of strain LSY42 (*BUD9/P_{GAL}-GFP-BUD9*) were grown to exponential phase in YM-P medium containing 2% raffinose instead of glucose. Galactose was added to 1% to induce expression of *GFP-BUD9,* and incubation was continued. After ~60 min, samples of cells were washed once with water, stained with 1 μg/ml Calcofluor as described in MATERIALS AND METHODS, and viewed for GFP (D and E) or Calcofluor (F; same cells as in E) fluorescence. Some cells are numbered for reference in the text. Arrows indicate birth scars.

Staining with Calcofluor revealed that all of the unbudded cells with GFP-Bud8p at both poles were daughter cells that had never budded (our unpublished results), and time-lapse analysis (Figure 9) revealed how this pattern of Bud8p localization was generated. For example, in panels 2 and 3, cell *a* had a large bud with a rather diffuse patch of GFP-Bud8p at its distal tip and no detectable GFP-Bud8p signal at its neck. Signal then appeared at the neck (panels 4–7), and when the mother and daughter cells separated (panel 8), most or all of this signal partitioned to the daughter cell. Cell *b* showed the same phenomena (panel 19 ff.). The time-lapse analysis also revealed several other features of interest. First, although the patches of GFP-Bud8p at incipient bud sites and on newly formed buds were quite tight (cell *b,* panel 3 ff.; cell *c,* panel 2 ff.; cell *d,* panel 8 ff.; cell *e,* panel 16 ff.), they became rather diffuse later in bud growth (cells *b* and *c,* panel 12 ff.). This explains why newborn daughter cells (e.g., cell *a*'s daughter, panel 8; cell *b*'s daughter, panel 23; also, presumably, cells *d* and *e,* panel 2) had diffuse patches of GFP-Bud8p at their distal poles and tight patches at their proximal poles. Second, the diffuse patches of GFP-Bud8p at the distal poles of newborn daughters became dramatically tighter during the several minutes just before bud emergence at that pole (cell *d,* panels 6–11; cell *e,* panels 12–18; this rapid tightening is particularly vivid in the accompanying movie).

In strains carrying a low-copy or high-copy *GFP-BUD9* plasmid, little or no signal was detected. However, when cells expressing *GFP-BUD9* under control of the *GAL* promoter were induced for ~1 h and then examined, a GFP signal could be detected in ~30% of the cells. In cells with medium-sized or large buds, GFP-Bud9p was typically observed at the mother-bud necks and appeared to be asymmetrically localized to the bud side of the neck (Figure 8D, cells 1–5). These concentrations of Bud9p appeared to remain in place during division, because unbudded cells typically showed a single patch of GFP-Bud9p at one pole of the cell (Figure 8E, cells 1–5), and staining with Calcofluor revealed that such cells were all daughter cells and that the GFP-Bud9p patches were at their proximal poles (Figure 8F). These results support the hypothesis that Bud9p is a component of the proximal-pole marker. Unexpectedly, however, GFP-Bud9p was also observed at the bud tips of some budded cells (Figure 8D, cells 5 and 6), including some cells with small buds (our unpublished results), as well as at both poles of some unbudded daughter cells (Figure 8E, cell 6). The proportion of cells with bud-tip localization of GFP-Bud9p increased with increasing times of expression in galactose medium.

Localization of Bud8p in Mutant and LatA-treated Cells

To explore some of the functional relationships among proteins involved in bipolar budding, we examined the localization of GFP-Bud8p in strains carrying mutations in sev-

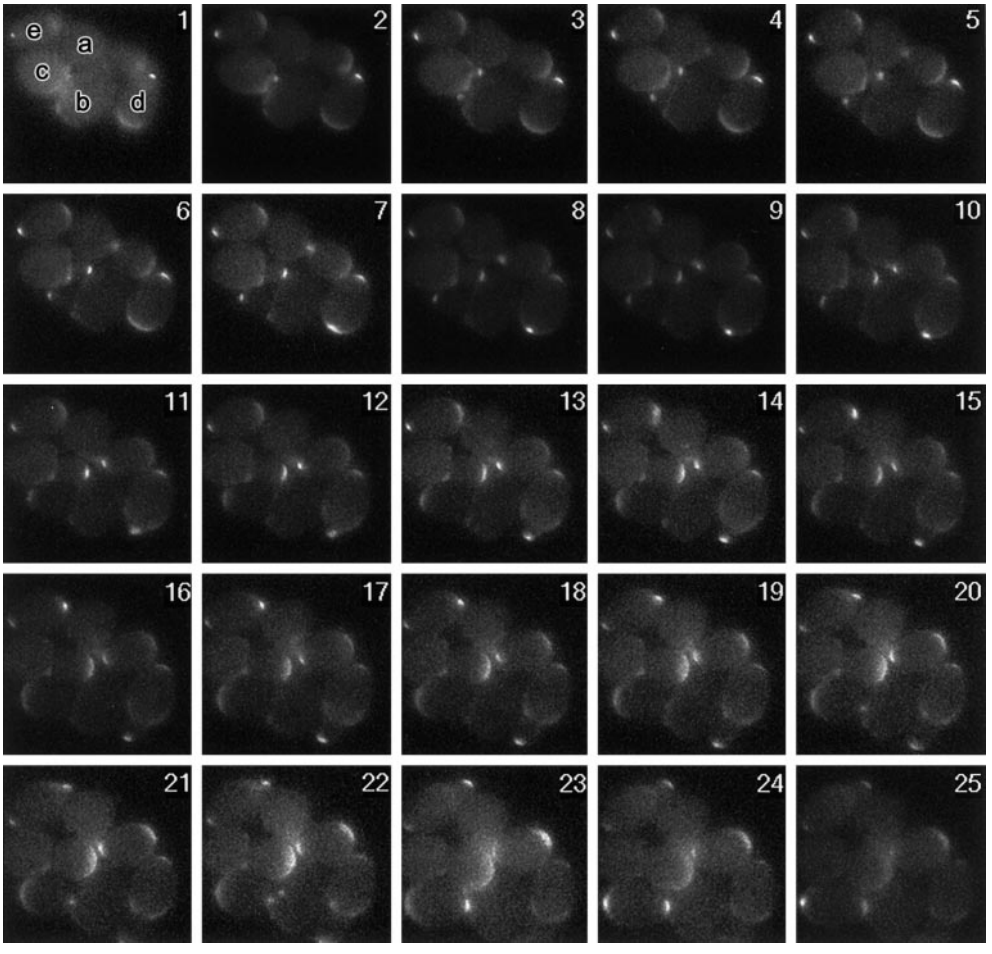

Figure 9. Time-lapse observations of GFP-Bud8p localization. Cells of *bud8*-Δ*1*/*bud8*-Δ*1* strain YHH415 carrying plasmid YEpGFP-BUD8 were grown and imaged as described in MATERIALS AND METHODS. Images were collected at 1-min intervals for 159 min. The figure shows every fourth image for 84 min (panels 1–22) followed by the images collected at 116, 124, and 128 min (panels 23–25, respectively). Some cells are marked for reference in the text. The entire image series can be accessed as a QuickTime movie.

eral other relevant genes. Because Bud9p does not appear to be involved in budding at the distal pole, it seemed unlikely that *bud9* mutations would affect the localization of Bud8p. Indeed, the distribution of GFP-Bud8p in a *bud9* deletion strain (Figure 10B) resembled that in wild-type cells (Figures 8, A–C, and 10A). In addition, although Rsr1p, Bud2p, and Bud5p are essential for bipolar (and axial) budding, these proteins are thought to function downstream of the spatial markers (see INTRODUCTION). Consistent with this model, the distribution of GFP-Bud8p in *rsr1* (strain AB324), *bud2* (strain YHH782), and *bud5* (strain YHH759) mutant cells was essentially the same as in wild-type cells (our unpublished results).

It was of particular interest to examine Bud8p localization in *bud6*, *spa2*, and *bni1* mutants. In diploid *bud6* or *spa2* mutant cells, the first buds appear to form more-or-less normally at the distal pole (Zahner *et al.*, 1996; Amberg *et al.*, 1997), although the positioning of subsequent bud sites is nearly random. (There are some subtle effects on the positions of the first buds that have been considered elsewhere [Zahner *et al.*, 1996; Amberg *et al.*, 1997; Sheu *et al.*, 2000].) These observations suggested that the localization of Bud8p would be approximately normal in these mutants. In contrast, diploid *bni1* mutants appear to bud in random locations in the first as well as in subsequent cell cycles (Zahner *et al.*, 1996), suggesting that Bud8p localization might be lost in a *bni1* mutant. Expression of GFP-Bud8p in appropriate mutant strains confirmed both of these expectations (Figure 10, C–F).

Bud6p and Spa2p are involved in the organization of the actin cytoskeleton (Amberg *et al.*, 1997; Fujiwara *et al.*, 1998; Sheu *et al.*, 1998; Jaquenoud and Peter, 2000). Mutations in several other genes that affect the actin cytoskeleton also produce bipolar-budding phenotypes similar to those of *bud6* and *spa2* mutants (Yang *et al.*, 1997). Taken together, these data suggested strongly that the delivery of the distal-pole marker was actin independent, a conclusion that seemed plausible given that a variety of proteins is known to arrive at the presumptive bud site in an actin-independent manner (Ayscough *et al.*, 1997). Although Bni1p is also involved in the organization of the actin cytoskeleton (Evangelista *et al.*, 1997; Fujiwara *et al.*, 1998; Bi *et al.*, 2000; Jaquenoud and Peter, 2000), it also interacts genetically with the septins (Fares and Pringle, unpublished data). Thus, a plausible interpretation of the loss of distal-pole budding (and of Bud8p localization) in *bni1* mutants was that the delivery of Bud8p to the presumptive bud site was septin dependent. Remarkably, however, Bud8p localization appears to be actin dependent and septin independent.

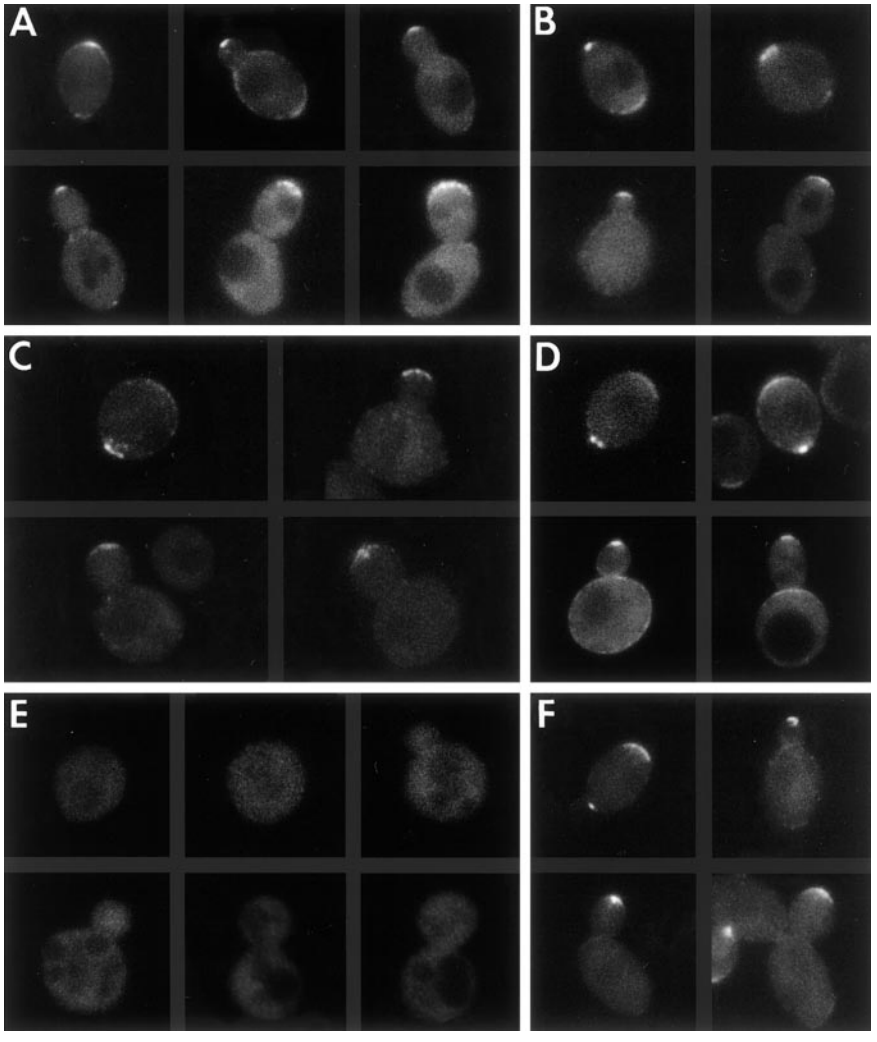

Figure 10. Localization of GFP-Bud8p in mutant strains. Cells of the indicated strains, all carrying plasmid YEpGFP-BUD8, were grown overnight on SC-Leu or SC-Leu-Ura plates, then suspended in water for viewing. (A) Wild-type strain YEF473; (B) *bud9-Δ1/bud9-Δ1* strain YHH615; (C) *bud6-Δ3/bud6-Δ3* strain YJZ358; (D) *spa2Δ3::URA3/spa2Δ3::URA3* strain YS148; (E) *bni1Δ::HIS3/bni1Δ::HIS3* strain YHH802; (F) *bni1Δ::HIS3/bni1Δ::HIS3* [p39L12] (a *BNI1* plasmid) strain YHH800.

To test for a possible role of actin, we used the inhibitor LatA, which produces a very rapid and essentially complete loss of filamentous actin (Ayscough *et al.*, 1997). Stationary-phase cells were mostly unbudded and devoid of incipient bud sites (as judged by septin staining), and they showed no detectable patches of GFP-Bud8p signal (Figure 11A, t = 0′). On resumption of growth in the absence of LatA, patches of GFP-Bud8p appeared at presumptive bud sites within 2 h (Figure 11A, t = 120′, DMSO). In contrast, in the presence of LatA, although incipient bud sites could be recognized by 120 min on the basis of their septin staining (as expected from the previous work of Ayscough *et al.*, 1997), no patches of GFP-Bud8p could be detected (Figure 11A, t = 120′, LatA). Thus, at least under these conditions, the delivery of Bud8p to the presumptive bud site appears to be actin dependent.

In contrast, when the possible septin dependence of Bud8p localization was evaluated with the use of the *cdc12-6* septin mutation (which causes a rapid and seemingly complete loss of septin organization upon shift to restrictive temperature: Adams and Pringle, 1984), it was clear not only that existing bud-tip patches of GFP-Bud8p could be maintained but that new patches of GFP-Bud8p could form at incipient bud sites (Figure 11B; note especially the new buds forming at 120 and 180 min). Thus, localization of Bud8p to the bud site and bud tip, and thus eventually to the distal pole of the daughter cell, appears to be septin independent. In contrast, GFP-Bud8p localization to the mother-bud neck was not observed in the septin mutant, although it was seen clearly in wild-type cells grown under the same conditions (Figure 11B, 60′). Thus, Bud8p localization to the neck, like that of most other proteins that localize to that site (Longtine *et al.*, 1996, 1998a, 2000; Longtine and Pringle, 1999), appears to be septin dependent.

DISCUSSION

Bud8p and Bud9p as the Apparent Markers of Bipolar Budding Sites

Despite some complications (discussed below), the results presented here suggest strongly that Bud8p and Bud9p are

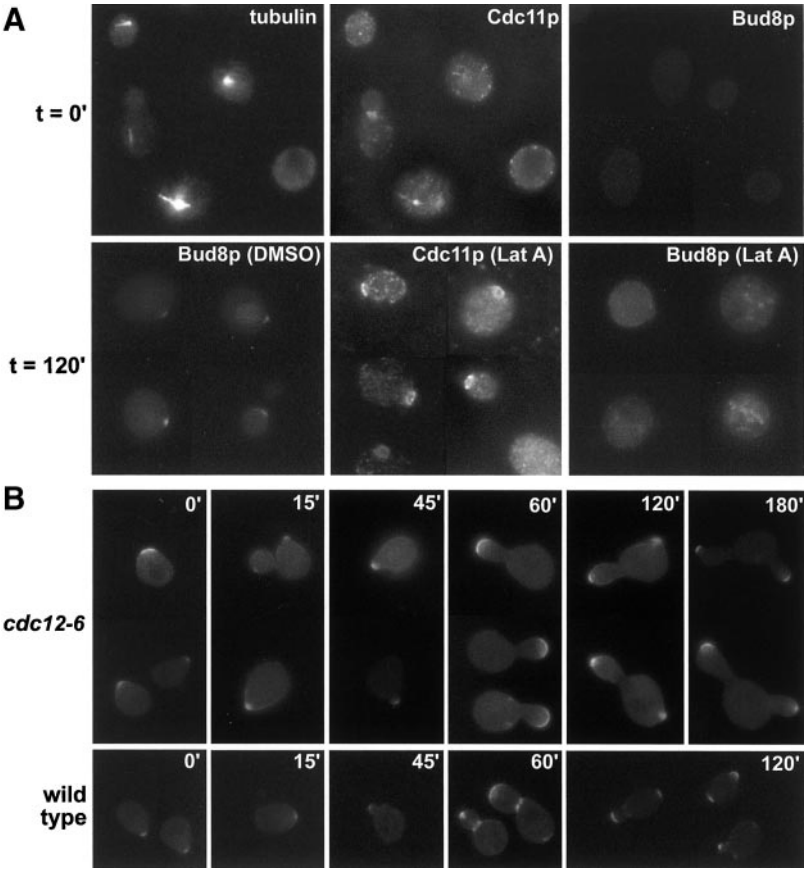

Figure 11. Dependence of Bud8p localization to the bud tip on actin but not on the septins. All strains contained plasmid YEpGFP∗-BUD8. (A) Strain YHH415 (*bud8*Δ/*bud8*Δ) was treated with LatA in DMSO or DMSO alone as described in MATERIALS AND METHODS. Samples taken at the beginning of the incubations with LatA or DMSO (t = 0′) and at intervals thereafter were examined for GFP fluorescence or fixed and processed for immunofluorescence using anti-tubulin antibodies (to demonstrate successful permeabilization of the stationary-phase cells for immunofluorescence) or anti-Cdc11p antibodies (to score for the presence of incipient bud sites). At t = 0′, most cells were unbudded and showed no localized septin staining; a few budded cells were present and showed septin staining at the neck, as expected. (B) Strains ML130 (wild type) and LSY192 (*cdc12-6*) were synchronized with α factor as described in MATERIALS AND METHODS. Samples taken at intervals after the release from α factor arrest at 37°C were examined for GFP fluorescence. Other samples taken at the same times were fixed and examined for septin localization by immunofluorescence using anti-Cdc11p antibodies; these observations verified that the septins localized normally in strain ML130 but were undetectable throughout the period of the experiment in strain LSY192, as expected.

essential components of the spatial markers for bipolar budding at the distal and proximal poles, respectively (Figure 12). Deletion of *BUD8* or *BUD9* has no detectable effect on the axial budding pattern, but diploid *bud8* deletion strains show an essentially complete loss of ability to bud at the distal pole, whereas diploid *bud9* deletion strains show an essentially complete loss of ability to bud at the proximal pole. Moreover, diploid *bud8 bud9* double-deletion strains bud in essentially random locations (when their ability to use axial budding cues is also disabled by deleting *BUD3*), and strains overexpressing *BUD8* or *BUD9* show either an enhanced use of the corresponding pole or a randomization of budding pattern (apparently depending on the level of expression). It should also be noted that Mösch and Fink (1997) identified transposon-insertion mutations in *BUD8* in a screen for mutants defective in pseudohyphal growth, which depends on budding at the distal poles of daughter cells (Gimeno *et al.*, 1992; Kron *et al.*, 1994).

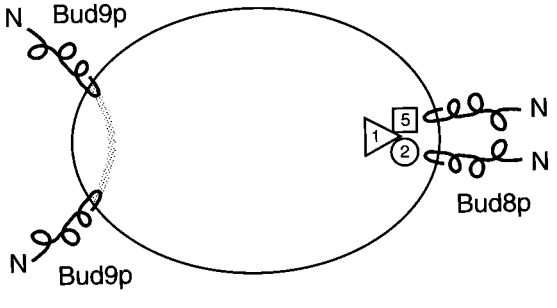

Figure 12. Proposed localization, membrane topology, and function of Bud8p and Bud9p. The cytoplasmic domain of Bud8p or Bud9p appears to be recognized (directly or indirectly) by Bud2p (circle) and Bud5p (square), the regulatory factors that control the Rsr1p GTPase (triangle), which in turn communicates positional information to the polarity-establishment proteins. See text for further discussion.

The apparent use of axial budding cues by diploid *bud8-Δ1 bud9-Δ1* cells was surprising, because axial budding appears to depend on Axl1p, whose expression is repressed in ***a***/α cells (Fujita *et al.*, 1994; Chant, 1999). Evidently, either *AXL1* is not completely repressed in ***a***/α cells or axial budding does not depend absolutely on Axl1p, so that when the bipolar budding markers are absent, the axial marker (whose known components are expressed in ***a***/α cells: Chant *et al.*, 1995; Halme *et al.*, 1996; Roemer *et al.*, 1996a; Sanders and Herskowitz, 1996) can be recognized with limited efficiency. These observations focus attention on the very interesting questions of how haploid cells normally use axial sites with such high fidelity (Madden and Snyder, 1992; Chant and Pringle, 1995), despite the apparent presence of all components needed for bipolar budding (Chant and Herskowitz, 1991; Madden and Snyder, 1992; Chant and Pringle,

1995), and of how diploid cells normally use bipolar sites with high fidelity despite their apparent ability to use axial cues if the bipolar ones are absent.

The structures and localizations of Bud8p and Bud9p also support the hypothesis that they mark the distal and proximal poles. Detailed analysis of the bipolar pattern had suggested that it depends on spatially and temporally persistent markers (Chant and Pringle, 1995). The apparent persistence of the markers led to the prediction that they might involve transmembrane proteins whose mobility is limited by interactions with the cell wall (Chant and Pringle, 1995). Bud8p and Bud9p appear to fit this prediction. Analyses of their sequences, their behaviors during fractionation, their glycosylation patterns, and their localizations all indicate that both Bud8p and Bud9p are integral plasma-membrane proteins, the bulk of whose mass (polypeptide plus attached *N*- and *O*-linked glycosyl moieties) is in the extracellular space (Figure 12). Although most of the data could be explained if only one of the hydrophobic domains in each protein were transmembrane, it seems more likely that both are and indeed that the two putative transmembrane domains actually associate with each other in the membrane; such an association might explain how a charge-exposing kink in the (presumed) transmembrane helix (caused by the pair of prolines [Figure 4A]) could be tolerated and thus might also explain the otherwise rather surprising conservation of sequence between the transmembrane domains of Bud8p and Bud9p.

Although we had little success in visualizing Bud8p or Bud9p localization without overexpression, our observations are mostly consistent with the postulated roles of these proteins. As expected (Chant and Pringle, 1995; Amberg *et al.*, 1997), Bud8p was found at presumptive bud sites, the tips of growing buds, and the distal poles of daughter cells, whereas Bud9p was observed at the bud side of the neck in large-budded cells and at the proximal poles of daughter cells. In addition, as expected (Zahner *et al.*, 1996; Amberg *et al.*, 1997; see RESULTS), Bud8p localization appeared approximately normal in *bud6* and *spa2* mutants but was undetectable in a *bni1* mutant. Surprisingly, however, in wild-type cells, we sometimes also observed Bud8p at the neck or the proximal pole of the daughter cell or Bud9p at the bud tip or the distal pole of the daughter cell. Although this point will require further investigation, we suspect that these observations are artifacts resulting from overexpression of the proteins: the mechanisms that direct these structurally similar proteins to their normal locations (see below) seem likely to be overwhelmed when the proteins are overproduced, causing each protein to be delivered to the location normal for the other as well to its own normal location. Consistent with this interpretation, the frequency of the putatively aberrant localization appeared to be higher when the levels of overexpression were greater (see RESULTS).

Although the extracytoplasmic domains of Bud8p and Bud9p have only very limited similarity in sequence, the cytoplasmic domains are very similar. This similarity may allow the cytoplasmic components of the bud-site-selection pathway to recognize essentially the same signal at the two poles of the cell. Although it is not known how this recognition occurs or whether the same components are involved at the two poles, the identification of special alleles of *BUD2* and *BUD5* that disable bipolar but not axial budding (Zahner *et al.*, 1996) suggests that Bud2p and Bud5p (which are regulatory elements of the Rsr1p module) may be directly involved (Figure 12). These observations do not appear to help solve (and indeed might be said to deepen) the mystery of why daughter cells show such a strong bias for forming their first few buds at the distal pole (Chant and Pringle, 1995; Zahner *et al.*, 1996; Figure 3A).

Other Unsolved Problems

Although the working model of Figure 12 seems likely to be correct at least in outline, it leaves many questions unanswered in addition to those already noted above. Some of these questions relate to the structures of Bud8p and Bud9p themselves. For example, it is not clear that the *N*- and *O*-linked glycosylation can fully account for the differences between the expected and observed electrophoretic mobilities of these proteins. It is possible that the deglycosylated polypeptides migrate atypically during SDS-PAGE. Alternatively, there may be residual *O*-linked glycosylation on Bud8p and/or Bud9p expressed in strains with the combinations of *pmt* mutations used in this study (Gentzsch and Tanner, 1996, 1997; Orlean, 1997; Sanders *et al.*, 1999), the proteins may have *N*-glycosyl moieties that are resistant to cleavage by the enzymes used (Van Rinsum *et al.*, 1991; Orlean, 1997), or both. Nonetheless, it also seems possible that Bud8p and Bud9p are also modified in some other way(s).

It is also unclear whether the glycosylation serves any specific role(s) in the function of the proteins. One plausible possibility is that the extended conformations expected to result from *O*-glycosylation (Jentoft, 1990) cause Bud8p and Bud9p to project through the periplasmic space and into intimate interaction with the cell wall; as noted above, such interaction could help to explain how the bipolar markers can apparently remain in place through multiple cell cycles. The interactions could be either with polysaccharide components of the wall or with one or more of the cell-wall proteins that are themselves linked to the polysaccharides (Orlean, 1997; Kapteyn *et al.*, 1999). In this regard, it is intriguing that not only the polysaccharide chitin but also some of the cell-wall proteins (Bony *et al.*, 1998; Ram *et al.*, 1998) have restricted spatial distributions.

However, these arguments also raise a difficult question: if Bud8p and Bud9p are really anchored in the cell wall, how can we explain the apparent movements of Bud8p (its apparent dispersion late in the cell cycle and coalescence just before bud emergence), as seen in Figure 9 and the accompanying movie? Although we cannot yet answer this question, it should be noted that the apparent dispersion of Bud8p may actually be an artifact (of the overexpression used, of gradual inactivation of the GFP, of cleavage followed by diffusion of the GFP moiety, or of some combination of these factors), and the apparent coalescence may actually be the delivery of a new bolus of Bud8p to the presumptive bud site (which is expected in any case, given that daughter cells do not always form their first buds at their distal poles).

Another important question is whether the distal-pole and proximal-pole markers consist of Bud8p and Bud9p alone or of these proteins in combination with others. Although Zahner *et al.* (1996) identified two *bud8* mutants and three *bud9* mutants, this screen was almost certainly not saturated,

particularly as mutations affecting the hypothetical Bud8p and Bud9p partners might not have such strong effects on the budding patterns. In this regard, the inability of Triton X-100 to solubilize Bud8p or Bud9p may be relevant. Although this inability could just reflect variations in the efficiency with which integral-membrane proteins are extracted by this detergent (Deshaies and Schekman, 1990; Roemer and Bussey, 1995; Jiang *et al.*, 1996; Lin *et al.*, 1998; Lodder *et al.*, 1999), it might also reflect association of Bud8p and Bud9p with other proteins in complexes that are not disrupted by Triton X-100.

Another very interesting question is how the structurally similar Bud8p and Bud9p proteins become localized to the opposite poles of the cell. Clearly, one possibility is that each polypeptide contains targeting signals that direct it (by unknown mechanisms) to the appropriate site. However, another attractive possibility is that localization depends primarily on time of expression during the cell cycle. Just before bud emergence, many proteins are delivered to the presumptive bud site and form a "cap" there and subsequently at the tip of the emerging bud (Lew and Reed, 1995; Pruyne and Bretscher, 2000a,b); the delivery is actin-dependent in some cases and actin-independent in others (Ayscough *et al.*, 1997). Thus, if vesicles containing Bud8p are available for delivery to the plasma membrane only at that time, Bud8p could arrive at the presumptive bud site as part of this general traffic. Similarly, late in the cell cycle, many of the "cap proteins" (plus some others) become relocalized to the neck region (Lew and Reed, 1995; Pruyne and Bretscher, 2000a,b); thus, if vesicles containing Bud9p are available for delivery to the plasma membrane only at that time, Bud9p could arrive at the neck region as part of this general traffic (although this hypothesis would not in itself explain the asymmetric distribution of Bud9p at the neck). Consistent with this model, it has been reported that both *BUD8* and *BUD9* mRNAs peak periodically during the cell cycle (Cho *et al.*, 1998; Spellman *et al.*, 1998). This model also suggests that overexpression (or mistimed expression) of either protein would result in its appearance at the site appropriate for the other, as we have apparently observed.

The experiments with LatA appear to establish that the Bud8p that will mark the distal pole of the daughter cell arrives at the presumptive bud site of the mother cell in an actin-dependent manner. These observations presumably mean that the effect of *bni1* mutations on distal-pole budding and the localization of Bud8p can be interpreted in terms of Bni1p's known role in the organization of the actin cytoskeleton and without invoking a connection to the septins (see RESULTS). However, the actin dependence of Bud8p localization also creates a real mystery: how can so many other mutations that perturb the actin cytoskeleton have little or no effect on distal-pole budding and Bud8p localization (see RESULTS)?

Possible Relevance to Other Organisms

Determining an appropriate axis is a central problem for all cells that must polarize or divide asymmetrically. It remains unclear whether the mechanisms used by *S. cerevisiae* cells to select bud sites have close parallels in other types of cells. In particular, no homologs of Bud8p or Bud9p have been identified as yet in other organisms (including, rather surprisingly, *Candida albicans*). Nonetheless, we suggest that the mechanism of generating a spatially and temporally persistent marker by anchoring a transmembrane protein in extracellular material has such obvious utility that it will also be found in other types of cells (or at least among other cells with cell walls). Such mechanisms could have arisen independently during evolution or even be homologous to that in *S. cerevisiae*, because the sequence constraints on the marker proteins seem likely to be weak (so that residual sequence homology could be difficult or impossible to detect). It will be interesting to seek such parallels as more is learned about the mechanisms for axis selection in other types of cells.

ACKNOWLEDGMENTS

We thank Ted Salmon and members of our laboratories (particularly Joe Zahner, Amos McKenzie III, G.J.P. Dijkgraaf, and A.M. Sdicu) for their interest, support, helpful discussions, and assistance with experiments; Peter Koetter for communicating partial *BUD9* sequence in advance of release; and W. Tanner for providing mutant strains. This work was supported by National Institutes of Health Grants GM-31006 (to J.R.P.) and GM-24364 (to E.D. Salmon), a National Sciences and Engineering Research Council operating grant (to H.B.), and the RJEG Trust.

REFERENCES

Adams, A.E.M., and Pringle, J.R. (1984). Relationship of actin and tubulin distribution to bud growth in wild-type and morphogenetic-mutant *Saccharomyces cerevisiae*. J. Cell Biol. *98*, 934–945.

Amberg, D.C., Zahner, J.E., Mulholland, J.W., Pringle, J.R., and Botstein, D. (1997). Aip3p/Bud6p, a yeast actin-interacting protein that is involved in morphogenesis and the selection of bipolar budding sites. Mol. Biol. Cell *8*, 729–753.

Ausubel, F.M., Brent, R., Kingston, R.E., Moore, D.D., Seidman, J.G., Smith, J.A., and Struhl, K. (1995). Current Protocols in Molecular Biology, New York: John Wiley & Sons.

Ayscough, K.R., Stryker, J., Pokala, N., Sanders, M., Crews, P., and Drubin, D.G. (1997). High rates of actin filament turnover in budding yeast and roles for actin in establishment and maintenance of cell polarity revealed using the actin inhibitor latrunculin-A. J. Cell Biol. *137*, 399–416.

Baudin, A., Ozier-Kalogeropoulos, O., Denouel, A., Lacroute, F., and Cullin, C. (1993). A simple and efficient method for direct gene deletion in *Saccharomyces cerevisiae*. Nucleic Acids Res. *21*, 3329–3330.

Bender, A., and Pringle, J.R. (1989). Multicopy suppression of the *cdc24* budding defect in yeast by *CDC42* and three newly identified genes including the *ras*-related gene. RSR1. Proc. Natl. Acad. Sci. USA *86*, 9976–9980.

Bi, E., and Pringle, J.R. (1996). *ZDS1* and *ZDS2*, genes whose products may regulate Cdc42p in *Saccharomyces cerevisiae*. Mol. Cell. Biol. *16*, 5264–5275.

Bi, E., Chiavetta, J.B., Chen, H., Chen, G.-C., Chan, C.S.M., and Pringle, J.R. (2000). Identification of novel, evolutionarily conserved Cdc42p-interacting proteins and of redundant pathways linking Cdc24p and Cdc42p to actin polarization in yeast. Mol. Biol. Cell *11*, 773–793.

Bony, M., Barre, P., and Blondin, B. (1998). Distribution of the flocculation protein, Flop, at the cell surface during yeast growth: the availability of Flop determines the flocculation level. Yeast *14*, 25–35.

Boone, C., Sommer, S.S., Hensel, A., and Bussey, H. (1990). Yeast *KRE* genes provide evidence for a pathway of cell wall β-glucan assembly. J. Cell Biol. *110*, 1833–1843.

Chant, J. (1999). Cell polarity in yeast. Annu. Rev. Cell Dev. Biol. *15*, 365–391.

Chant, J., Corrado, K., Pringle, J.R., and Herskowitz, I. (1991). Yeast *BUD5*, encoding a putative GDP-GTP exchange factor, is necessary for bud site selection and interacts with bud formation gene *BEM1*. Cell *65*, 1213–1224.

Chant, J., and Herskowitz, I. (1991). Genetic control of bud site selection in yeast by a set of gene products that constitute a morphogenetic pathway. Cell *65*, 1203–1212.

Chant, J., Mischke, M., Mitchell, E., Herskowitz, I., and Pringle, J.R. (1995). Role of Bud3p in producing the axial budding pattern of yeast. J. Cell Biol. *129*, 767–778.

Chant, J., and Pringle, J.R. (1995). Patterns of bud-site selection in the yeast *Saccharomyces cerevisiae*. J. Cell Biol. *129*, 751–765.

Cho, R.J., Campbell, M.J., Winzeler, E.A., Steinmetz, L., Conway, A., Wodicka, L., Wolfsberg, T.G., Gabrielian, A.E., Landsman, D., Lockhart, D.J., and Davis, R.W. (1998). A genome-wide transcriptional analysis of the mitotic cell cycle. Mol. Cell *2*, 65–73.

Christianson, T.W., Sikorski, R.S., Dante, M., Shero, J.H., and Hieter, P. (1992). Multifunctional yeast high-copy-number shuttle vectors. Gene *110*, 119–122.

Cormack, B.P., Valdivia, R.H., and Falkow, S. (1996). FACS-optimized mutants of the green fluorescent protein (GFP). Gene *173*, 33–38.

Deshaies, R.J., and Schekman, R. (1990). Structural and functional dissection of Sec62p, a membrane-bound component of the yeast endoplasmic reticulum protein import machinery. Mol. Cell. Biol. *10*, 6024–6035.

Drubin, D.G., and Nelson, W.J. (1996). Origins of cell polarity. Cell *84*, 335–344.

Esmon, P.C., Esmon, B.E., Schauer, I.E., Taylor, A., and Schekman, R. (1987). Structure, assembly, and secretion of octameric invertase. J. Biol. Chem. *262*, 4387–4394.

Evangelista, M., Blundell, K., Longtine, M.S., Chow, C.J., Adames, N., Pringle, J.R., Peter, M., and Boone, C. (1997). Bni1p, a yeast formin linking Cdc42p and the actin cytoskeleton during polarized morphogenesis. Science *276*, 118–122.

Ford, S.K., and Pringle, J.R. (1991). Cellular morphogenesis in the *Saccharomyces cerevisiae* cell cycle: localization of the *CDC11* gene product and the timing of events at the budding site. Dev. Genet. *12*, 281–292.

Foreman, P.K., and Davis, R.W. (1994). Cloning vectors for the synthesis of epitope-tagged, truncated and chimeric proteins in *Saccharomyces cerevisiae*. Gene *144*, 63–68.

Freifelder, D. (1960). Bud position in *Saccharomyces cerevisiae*. J. Bacteriol. *80*, 567–568.

Fujiki, Y., Hubbard, A.L., Fowler, S., and Lazarow, P.B. (1982). Isolation of intracellular membranes by means of sodium carbonate treatment: application to endoplasmic reticulum. J. Cell Biol. *93*, 97–102.

Fujita, A., Oka, C., Arikawa, Y., Katagai, T., Tonouchi, A., Kuhara, S., and Misumi, Y. (1994). A yeast gene necessary for bud-site selection encodes a protein similar to insulin-degrading enzymes. Nature *372*, 567–570.

Fujiwara, T., Tanaka, K., Mino, A., Kikyo, M., Takahashi, K., Shimizu, K., and Takai, Y. (1998). Rho1p-Bni1p-Spa2p interactions: implication in localization of Bni1p at the bud site and regulation of the actin cytoskeleton in *Saccharomyces cerevisiae*. Mol. Biol. Cell *9*, 1221–1233.

Gehrung, S., and Snyder, M. (1990). The *SPA2* gene of *Saccharomyces cerevisiae* is important for pheromone-induced morphogenesis and efficient mating. J. Cell Biol. *111*, 1451–1464.

Gentzsch, M., and Tanner, W. (1996). The *PMT* gene family: protein *O*-glycosylation in *Saccharomyces cerevisiae* is vital. EMBO J. *15*, 5752–5759.

Gentzsch, M., and Tanner, W. (1997). Protein-*O*-glycosylation in yeast: protein-specific mannosyltransferases. Glycobiology *7*, 481–486.

Gietz, D., St. Jean, A., Woods, R.A., and Schiestl, R.H. (1992). Improved method for high efficiency transformation of intact yeast cells. Nucleic Acids Res. *20*, 1425–1426.

Gietz, R.D., and Sugino, A. (1988). New yeast-*Escherichia coli* shuttle vectors constructed with in vitro mutagenized yeast genes lacking six-base pair restriction sites. Gene *74*, 527–534.

Gimeno, C.J., Ljungdahl, P.O., Styles, C.A., and Fink, G.R. (1992). Unipolar cell divisions in the yeast *S. cerevisiae* lead to filamentous growth: regulation by starvation and. RAS. Cell *68*, 1077–1090.

Goud, B., Salminen, A., Walworth, N.C., and Novick, P.J. (1988). A GTP-binding protein required for secretion rapidly associates with secretory vesicles and the plasma membrane in yeast. Cell. *53*, 753–768.

Guthrie, C., and Fink, G.R., ed. (1991). Guide to Yeast Genetics and Molecular Biology. Methods in Enzymology, vol 194, San Diego: Academic Press.

Halme, A., Michelitch, M., Mitchell, E.L., and Chant, J. (1996). Bud10p directs axial cell polarization in budding yeast and resembles a transmembrane receptor. Curr. Biol. *6*, 570–579.

Hartmann, E., Rapoport, T.A., and Lodish, H.F. (1989). Predicting the orientation of eukaryotic membrane-spanning proteins. Proc. Natl. Acad. Sci. USA *86*, 5786–5790.

Heim, R., Cubitt, A.B., and Tsien, R.Y. (1995). Improved green fluorescence. Nature *373*, 663–664.

Hicks, J.B., Strathern, J.N., and Herskowitz, I. (1977). Interconversion of yeast mating types. III. Action of the homothallism (*HO*) gene in cells homozygous for the mating type locus. Genetics *85*, 395–405.

Hofmann, K., and Stoffel, W. (1993). A database of membrane spanning protein segments. Biol. Chem. Hoppe-Seyler *374*, 166.

Jaquenoud, M., and Peter, M. (2000). Gic2p may link activated Cdc42p to components involved in actin polarization, including Bni1p and Bud6p (Aip3p). Mol. Cell. Biol. *20*, 6244–6258.

Jentoft, N. (1990). Why are proteins *O*-glycosylated? Trends Biochem. Sci. *15*, 291–294.

Jiang, B., Sheraton, J., Ram, A.F.J., Dijkgraaf, G.J.P., Klis, F.M., and Bussey, H. (1996). *CWH41* encodes a novel endoplasmic reticulum membrane *N*-glycoprotein involved in β1,6-glucan assembly. J. Bacteriol. *178*, 1162–1171.

Jones, J.S., and Prakash, L. (1990). Yeast *Saccharomyces cerevisiae* selectable markers in pUC18 polylinkers. Yeast *6*, 363–366.

Kapteyn, J.C., Van Den Ende, H., and Klis, F.M. (1999). The contribution of cell wall proteins to the organization of the yeast cell wall. Biochim. Biophys. Acta *1426*, 373–383.

Kilmartin, J.V., and Adams, A.E.M. (1984). Structural rearrangements of tubulin and actin during the cell cycle of the yeast *Saccharomyces cerevisiae*. J. Cell Biol. *98*, 922–933.

Koerner, T.J., Hill, J.E., Myers, A.M., and Tzagoloff, A. (1991). High-expression vectors with multiple cloning sites for construction of trpE fusion genes: pATH vectors. Methods Enzymol. *194*, 477–490.

Kron, S.J., Styles, C.A., and Fink, G.R. (1994). Symmetric cell division in pseudohyphae of the yeast *Saccharomyces cerevisiae*. Mol. Biol. Cell *5*, 1003–1022.

Kyte, J., and Doolittle, R.F. (1982). A simple method for displaying the hydropathic character of a protein. J. Mol. Biol. *157*, 105–132.

Laemmli, U.K. (1970). Cleavage of structural proteins during the assembly of the head of bacteriophage T4. Nature *227*, 680–685.

Lew, D.J., and Reed, S.I. (1995). Cell cycle control of morphogenesis in budding yeast. Curr. Opin. Genet. Dev. *5*, 17–23.

Lillie, S.H., and Pringle, J.R. (1980). Reserve carbohydrate metabolism in *Saccharomyces cerevisiae*: responses to nutrient limitation. J. Bacteriol. *143*, 1384–1394.

Lin, S., Naim, H.Y., Chapin Rodriguez, A., and Roth, M.G. (1998). Mutations in the middle of the transmembrane domain reverse the polarity of transport of the influenza virus hemagglutinin in MDCK epithelial cells. J. Cell Biol. *142*, 51–57.

Ljungdahl, P.O., Gimeno, C.J., Styles, C.A., and Fink, G.R. (1992). *SHR3*: a novel component of the secretory pathway specifically required for localization of amino acid permeases in yeast. Cell *71*, 463–478.

Lodder, A.L., Lee, T.K., and Ballester, R. (1999). Characterization of the Wsc1 protein, a putative receptor in the stress response of *Saccharomyces cerevisiae*. Genetics *152*, 1487–1499.

Longtine, M.S., DeMarini, D.J., Valencik, M.L., Al-Awar, O.S., Fares, H., De Virgilio, C., and Pringle, J.R. (1996). The septins: roles in cytokinesis and other processes. Curr. Opin. Cell Biol. *8*, 106–119.

Longtine, M.S., Fares, H., and Pringle, J.R. (1998a). Role of the yeast Gin4p protein kinase in septin assembly and the relationship between septin assembly and septin function. J. Cell Biol. *143*, 719–736.

Longtine, M.S., McKenzie, A.III, DeMarini, D.J., Shah, N.G., Wach, A., Brachat, A., Philippsen, P., and Pringle, J.R. (1998b). Additional modules for versatile and economical PCR-based gene deletion and modification in *Saccharomyces cerevisiae*. Yeast *14*, 953–961.

Longtine, M.S., and Pringle, J.R. (1999). Septins. In: Guidebook to the Cytoskeletal and Motor Proteins, eds. T. Kreis and R. Vale, Oxford, England: Oxford University Press, 359–363.

Longtine, M.S., Theesfeld, C.L., McMillan, J.N., Weaver, E., Pringle, J.R., and Lew, D.J. (2000). Septin-dependent assembly of a cell cycle-regulatory module in *Saccharomyces cerevisiae*. Mol. Cell. Biol. *20*, 4049–4061.

Lussier, M., Gentzsch, M., Sdicu, A.-M., Bussey, H., and Tanner, W. (1995). Protein *O*-glycosylation in yeast. The *PMT2* gene specifies a second protein *O*-mannosyltransferase that functions in addition to the *PMT1*-encoded activity. J. Biol. Chem. *270*, 2770–2775.

Lussier, M., Sdicu, A.-M., Bussereau, F., Jacquet, M., and Bussey, H. (1997a). The Ktr1p, Ktr3p, and Kre2p/Mnt1p mannosyltransferases participate in the elaboration of yeast *O*- and *N*-linked carbohydrate chains. J. Biol. Chem. *272*, 15527–15531.

Lussier, M., Sdicu, A.-M., Camirand, A., and Bussey, H. (1996). Functional characterization of the *YUR1, KTR1,* and *KTR2* genes as members of the yeast *KRE2/MNT1* mannosyltransferase gene family. J. Biol. Chem. *271*, 11001–11008.

Lussier, M., White, A.-M., Sheraton, J., di Paolo, T., Treadwell, J., Southard. S.B., Horenstein, C.I., Chen-Weiner, J., Ram, A.F.J., Kapteyn, J.C., Roemer, T.W., Vo, D.H., Bondoc, D.C., Hall, J., Zhong, W.W., Sdicu, A.-M., Davies, J., Klis, F.M., Robbins, P.W., and Bussey, H. (1997b). Large scale identification of genes involved in cell surface biosynthesis and architecture in *Saccharomyces cerevisiae*. Genetics *147*, 435–450.

Madden, K., and Snyder, M. (1992). Specification of sites for polarized growth in *Saccharomyces cerevisiae* and the influence of external factors on site selection. Mol. Biol. Cell *3,* 1025–1035.

Mösch, H.-U., and Fink, G.R. (1997). Dissection of filamentous growth by transposon mutagenesis in *Saccharomyces cerevisiae*. Genetics *145*, 671–684.

Nakayama, K., Nagasu, T., Shimma, Y., Kuromitsu, J., and Jigami, Y. (1992). *OCH1* encodes a novel membrane bound mannosyltransferase: outer chain elongation of asparagine-linked oligosaccharides. EMBO J. *11*, 2511–2519.

Orlean, P. (1997). Biogenesis of yeast wall and surface components. In: The Molecular and Cellular Biology of the Yeast *Saccharomyces.* Cell Cycle and Cell Biology, eds. J.R. Pringle, J.R. Broach, and E.W. Jones, Cold Spring Harbor, NY: Cold Spring Harbor Laboratory Press, 229–362.

Pringle, J.R., Adams, A.E.M., Drubin, D.G., and Haarer, B.K. (1991). Immunofluorescence methods for yeast. Methods Enzymol. *194*, 565–602.

Pringle, J.R., Bi, E., Harkins, H.A., Zahner, J.E., De Virgilio, C., Chant, J., Corrado, K., and Fares, H. (1995). Establishment of cell polarity in yeast. Cold Spring Harbor Symp. Quant. Biol. *60*, 729–743.

Pringle, J.R., Preston, R.A., Adams, A.E.M., Stearns, T., Drubin, D.G., Haarer, B.K., and Jones, E.W. (1989). Fluorescence microscopy methods for yeast. Methods Cell Biol. *31*, 357–435.

Pruyne, D., and Bretscher, A. (2000a). Polarization of cell growth in yeast. I. Establishment and maintenance of polarity states. J. Cell Sci. *113*, 365–375.

Pruyne, D., and Bretscher, A. (2000b). Polarization of cell growth in yeast. II. The role of the cortical actin cytoskeleton. J. Cell Sci. *113*, 571–585.

Ram, A.F.J., Wolters, A., Ten Hoopen, R., and Klis, F.M. (1994). A new approach for isolating cell wall mutants in *Saccharomyces cerevisiae* by screening for hypersensitivity to Calcofluor White. Yeast *10*, 1019–1030.

Ram, A.F.J., Van Den Ende, H., and Klis, F.M. (1998). Green fluorescent protein-cell wall fusion proteins are covalently incorporated into the cell wall of *Saccharomyces cerevisiae*. FEMS Microbiol. Lett. *162*, 249–255.

Reddy, V.A., Johnson, R.S., Biemann, K., Williams, R.S., Ziegler, F.D., Trimble, R.B., and Maley, F. (1988). Characterization of the glycosylation sites in yeast external invertase. I. *N*-linked oligosaccharide content of the individual sequons. J. Biol. Chem. *263*, 6978–6985.

Reid, B.J., and Hartwell, L.H. (1977). Regulation of mating in the cell cycle of *Saccharomyces cerevisiae*. J. Cell Biol. *75*, 355–365.

Riles, L., Dutchik, J.E., Baktha, A., McCauley, B.K., Thayer, B.C., Leckie, M.P., Braden, V.V., Depke, J.E., and Olson, M.V. (1993). Physical maps of the six smallest chromosomes of *Saccharomyces cerevisiae* at a resolution of 2.6 kilobase pairs. Genetics *134*, 81–150.

Robinson, J.S., Klionsky, D.J., Banta, L.M., and Emr, S.D. (1988). Protein sorting in *Saccharomyces cerevisiae*: isolation of mutants defective in the delivery and processing of multiple vacuolar hydrolases. Mol. Cell. Biol. *8*, 4936–4948.

Roemer, T., and Bussey, H. (1991). Yeast β-glucan synthesis: *KRE6* encodes a predicted type II membrane protein required for glucan synthesis *in vivo* and for glucan synthase activity *in vitro*. Proc. Natl. Acad. Sci. USA *88*, 11295–11299.

Roemer, T., and Bussey, H. (1995). Yeast Kre1p is a cell surface. O-glycoprotein. Mol. Gen. Genet. *249*, 209–216.

Roemer, T., Madden, K., Chang, J., and Snyder, M. (1996a). Selection of axial growth sites in yeast requires Axl2p, a novel plasma membrane glycoprotein. Genes Dev. *10*, 777–793.

Roemer, T., Paravicini, G., Payton, M.A., and Bussey, H. (1994). Characterization of the yeast (1→6)-β-glucan biosynthetic components, Kre6p and Skn1p, and genetic interactions between the *PKC1* pathway and extracellular matrix assembly. J. Cell Biol. *127*, 567–579.

Roemer, T., Vallier, L.G., and Snyder, M. (1996b). Selection of polarized growth sites in yeast. Trends Cell Biol. *6*, 434–441.

Sääf, A., Johansson, M., Wallin, E., and von Heijne, G. (1999). Divergent evolution of membrane protein topology: the *Escherichia coli* RnfA and RnfE homologues. Proc. Natl. Acad. Sci. USA *96*, 8540–8544.

Salmon, E.D., Yeh, E., Shaw, S., Skibbens, B., and Bloom, K. (1998). High-resolution video and digital-enhanced differential interference contrast light microscopy of cell division in budding yeast. Methods Enzymol. *298*, 317–331.

Sambrook, J., Fritsch, E.F., and Maniatis, T. (1989). Molecular Cloning: A Laboratory Manual, Cold Spring Harbor, NY: Cold Spring Harbor Laboratory Press.

Sanders, S.L., and Herskowitz, I. (1996). The Bud4 protein of yeast, required for axial budding, is localized to the mother/bud neck in a cell cycle-dependent manner. J. Cell Biol. *134*, 413–427.

Sanders, S.L., Gentzsch, M., Tanner, W., and Herskowitz, I. (1999). *O*-glycosylation of Axl2p/Bud10p by Pmt4p is required for its stability, localization, and function in daughter cells. J. Cell Biol. *145*, 1177–1188.

Schneider, B.L., Seufert, W., Steiner, B., Yang, Q.H., and Futcher, A.B. (1995). Use of polymerase chain reaction epitope tagging for protein tagging in *Saccharomyces cerevisiae*. Yeast *11*, 1265–1274.

Shahinian, S., Dijkgraaf, G.J.P., Sdicu, A.-M., Thomas, D.Y., Jakob, C.A., Aebi, M., and Bussey, H. (1998). Involvement of protein *N*-glycosyl chain glucosylation and processing in the biosynthesis of cell wall β-1,6-glucan of *Saccharomyces cerevisiae*. Genetics *149*, 843–856.

Sheu, Y.-J., Barral, Y., and Snyder, M. (2000). Polarized growth controls cell shape and bipolar bud site selection in *Saccharomyces cerevisiae*. Mol. Cell. Biol. *20*, 5235–5247.

Sheu, Y.-J., Santos, B., Fortin, N., Costigan, C., and Snyder, M. (1998). Spa2p interacts with cell polarity proteins and signaling components involved in yeast cell morphogenesis. Mol. Cell. Biol. *18*, 4053–4069.

Sikorski, R.S., and Hieter, P. (1989). A system of shuttle vectors and yeast host strains designed for efficient manipulation of DNA in *Saccharomyces cerevisiae*. Genetics *122*, 19–27.

Spellman, P.T., Sherlock, G., Zhang, M.Q., Iyer, V.R., Anders, K., Eisen, M.B., Brown, P.O., Botstein, D., and Futcher, B. (1998). Comprehensive identification of cell cycle-regulated genes of the yeast *Saccharomyces cerevisiae* by microarray hybridization. Mol. Biol. Cell *9*, 3273–3297.

Straight, A.F., Sedat, J.W., and Murray, A.W. (1998). Time-lapse microscopy reveals unique roles for kinesins during anaphase in budding yeast. J. Cell Biol. *143*, 687–694.

Tanner, W., and Lehle, L. (1987). Protein glycosylation in yeast. Biochim. Biophys. Acta *906*, 81–99.

Tyers, M., Tokiwa, G., and Futcher, B. (1993). Comparison of the *Saccharomyces cerevisiae* G_1 cyclins: Cln3 may be an upstream activator of Cln1, Cln2 and other cyclins. EMBO J. *12*, 1955–1968.

Van Rinsum, J., Klis, F.M., and Van Den Ende, H. (1991). Cell wall glucomannoproteins of *Saccharomyces cerevisiae mnn9*. Yeast *7*, 717–726.

von Heijne, G. (1996). Principles of membrane protein assembly and structure. Prog. Biophys. Mol. Biol. *66*, 113–139.

Yang, S., Ayscough, K.R., and Drubin, D.G. (1997). A role for the actin cytoskeleton of *Saccharomyces cerevisiae* in bipolar bud-site selection. J. Cell Biol. *136*, 111–123.

Yip, C.L., Welch, S.K., Klebl, F., Gilbert, T., Seidel, P., Grant, F.J., O'Hara, P.J., and MacKay, V.L. (1994). Cloning and analysis of the *Saccharomyces cerevisiae MNN9* and *MNN1* genes required for complex glycosylation of secreted proteins. Proc. Natl. Acad. Sci. USA *91*, 2723–2727.

Zahner, J.E., Harkins, H.A., and Pringle, J.R. (1996). Genetic analysis of the bipolar pattern of bud site selection in the yeast *Saccharomyces cerevisiae*. Mol. Cell. Biol. *16*, 1857–1870.